Chapter 5
Detection of Known Signals in Noise

The performance of a communication link is degraded by many transmission impairments including fading, delay spread, Doppler spread, co-channel and adjacent channel interference, noise, and receiver implementation losses. Fading causes a very low instantaneous received signal-to-noise ratio (SNR) or carrier-to-noise ratio (CNR) when the channel exhibits a deep fade, delay spread causes intersymbol interference (ISI) between the transmitted symbols, and a large Doppler spread is indicative of rapid channel variations and may necessitate a receiver with a fast convergent algorithm. Receiver implementation losses include carrier frequency offset, sample clock frequency offset, symbol timing errors, and channel estimation errors. Co-channel interference, adjacent channel interference, and noise are additive impairments that degrade the bit error rate performance by reducing the SNR or CNR.

This chapter considers the bit error rate performance of digital signaling on frequency non-selective (flat) fading channels with additive white Gaussian noise AWGN. Flat fading channels are characteristic of narrow-band land mobile radio systems or mobile satellite systems. Flat fading channels affect all frequency components of a narrow-band signal in exactly the same way and, therefore, do not introduce amplitude or phase distortion into the waveform that is transmitted over the communication link. Frequency selective channels, on the other hand, distort the transmitted signal and will be the subject of Chap. 7. Flat fading channels will be shown to significantly degrade the bit error rate performance unless appropriate countermeasures are taken. Diversity and coding are two well-known methods for combating fading. The basic idea of diversity systems is to provide the receiver with multiple replicas of the same information bearing signal, where the replicas are affected by uncorrelated fading. This can be accomplished by using multiple receiver antennas with sufficient spatial separation, for example. Multi-antenna techniques will be discussed in Chap. 6. Coding techniques introduce a form of time diversity into the transmitted signal which, along with interleaving, can be exploited to mitigate the effects of fading. Coding techniques are the topic of Chap. 8.

The remainder of this chapter is organized as follows. Section 5.1 introduces a vector representation for digital signaling on flat fading channels with additive white Gaussian noise (AWGN). Section 5.3 provides a generalized analysis of the error rate performance of digital signaling on flat fading channels. Section 5.2 derives the structure of the optimum coherent receiver for the detection of known signals in AWGN. The error probability performance of various coherently detected digital signaling schemes is considered, including PSK in Sect. 5.4, QAM in Sect. 5.5, orthogonal signals in Sect. 5.6, and OFDM in Sect. 5.7. Section 5.8 considers differential detection of DPSK and $\pi/4$-DQPSK waveforms. Section 5.9 considers non-coherent detection and, finally, Sect. 5.10 considers coherent and non-coherent detection of CPM waveforms.

5.1 Vector Space Representation of Received Signals

Consider a general digital modulation scheme having the complex envelope

$$\tilde{s}(t) = A \sum_{n} b(t - nT, \mathbf{x}_n), \tag{5.1}$$

where the generalized shaping function $b(t-nT, \mathbf{x}_n)$ depends on the particular modulation scheme being employed. Suppose the waveform $\tilde{s}(t)$ is transmitted over a flat fading channel having the time-variant channel impulse response

G.L. Stüber, *Principles of Mobile Communication*, DOI 10.1007/978-3-319-55615-4_5

$$g(t,\tau) = g(t)\delta(\tau - \hat{\tau}). \tag{5.2}$$

The received complex envelope is

$$\tilde{r}(t) = g(t)\tilde{s}(t - \hat{\tau}) + \tilde{n}(t), \tag{5.3}$$

where $g(t) = \alpha(t)e^{j\phi(t)}$ is the time-variant complex fading gain introduced by the channel, and $\tilde{n}(t)$ is zero-mean complex additive white Gaussian noise (AWGN) with a power spectral density (psd) of N_o watts/Hz. Note that the fading channel introduces a multiplicative distortion, while the receiver front end introduces AWGN. The flat fading channel will also introduce a random time delay $\hat{\tau}$.

Consider a linear full response modulation scheme, such as QAM or PSK, where one of M message waveforms having a complex envelope chosen from the set $\{\tilde{s}_i(t)\}_{i=1}^{M}$ is transmitted over a flat fading channel every T seconds. By observing received waveform $\tilde{r}(t)$, the receiver must determine the time sequence of message waveforms that was transmitted over the channel. To do so, the receiver must determine the time delay $\hat{\tau}$, such that the location of the symbol boundaries in the received waveform are known. The process of estimating $\hat{\tau}$ is commonly called symbol or baud timing recovery. For our present purpose, it is assumed that the receiver knows $\hat{\tau}$ exactly and, therefore, it can be assumed that $\hat{\tau} = 0$. Under the above assumptions, the received complex envelope can be written as

$$\tilde{r}(t) = g(t)\tilde{s}(t) + \tilde{n}(t). \tag{5.4}$$

To derive the structure of the optimum coherent receiver, suppose that a single isolated message waveform $\tilde{s}_n(t)$ is chosen from the set $\{\tilde{s}_i(t)\}_{i=1}^{M}$ and transmitted over the channel. If the channel changes very slowly with respect to the symbol period T, i.e., $f_m T \ll 1$, then $g(t)$ will remain essentially constant over the duration of the amplitude shaping pulse $h_a(t)$. Under this condition, the explicit time dependency of $g(t)$ can be removed so that the received complex envelope is

$$\tilde{r}(t) = g\tilde{s}_n(t) + \tilde{n}(t), \tag{5.5}$$

where $g = \alpha e^{j\phi}$ is the random fading gain.

Chapter 4 showed that the set of waveforms $\{\tilde{s}_i(t)\}_{i=1}^{M}$ can be represented as a set vectors $\{\tilde{\mathbf{s}}_i\}_{i=1}^{M}$ in an N-dimensional signal space. The signal vectors and the associated basis functions, $\{\varphi_i(t)\}_{i=1}^{N}$ may be obtained by using a Gram–Schmidt orthonormalization procedure. To derive the structure of the optimal coherent receiver, it is useful to obtain a vector representation of the received waveform in (5.5). This can be accomplished by projecting the received complex envelope $\tilde{r}(t)$ onto the set of basis functions $\{\varphi_i(t)\}_{i=1}^{N}$ giving the representation

$$\tilde{r}(t) = \sum_{i=1}^{N} \tilde{r}_i \varphi_i(t) + \tilde{z}(t), \tag{5.6}$$

where

$$\tilde{r}_i = \int_{-\infty}^{\infty} \tilde{r}(t)\varphi_i^*(t)\mathrm{d}t \tag{5.7}$$

$$= g\int_{-\infty}^{\infty} \tilde{s}_n(t)\varphi_i^*(t)\mathrm{d}t + \int_{-\infty}^{\infty} \tilde{n}(t)\varphi_i^*(t)\mathrm{d}t \tag{5.8}$$

$$= g\tilde{s}_{n_i} + \tilde{n}_i \tag{5.9}$$

and

$$\tilde{z}(t) = \tilde{n}(t) - \sum_{i=1}^{N} \tilde{n}_i \varphi_i(t) \tag{5.10}$$

is a "remainder" process, which is the portion of the noise process $\tilde{n}(t)$ that lies outside of the signal space. The above process yields the received vector

$$\tilde{\mathbf{r}} = g\tilde{\mathbf{s}}_n + \tilde{\mathbf{n}}, \tag{5.11}$$

where

$$\tilde{\mathbf{r}} = (\tilde{r}_1, \tilde{r}_2, \ldots, \tilde{r}_N)$$
$$\tilde{\mathbf{s}}_n = (\tilde{s}_{n_1}, \tilde{s}_{n_2}, \ldots, \tilde{s}_{n_N})$$
$$\tilde{\mathbf{n}} = (\tilde{n}_1, \tilde{n}_2, \ldots, \tilde{n}_N).$$

For an AWGN channel, the $\tilde{n}_k, k = 1, \ldots, N$ are complex Gaussian random variables that can be completely described by their means and covariances. The means are

$$\mathrm{E}[\tilde{n}_k] = \int_{-\infty}^{\infty} \mathrm{E}[\tilde{n}(t)]\varphi_k(t)\mathrm{d}t = 0 \tag{5.12}$$

and covariances are[1]

$$\begin{aligned}\phi_{\tilde{n}_j\tilde{n}_k} = \frac{1}{2}\mathrm{E}[\tilde{n}_j\tilde{n}_k^*] &= \int_{-\infty}^{\infty}\int_{-\infty}^{\infty}\frac{1}{2}\mathrm{E}[\tilde{n}(t)\tilde{n}^*(s)]\varphi_j(t)\varphi_k^*(s)\mathrm{d}t\mathrm{d}s \\ &= N_o\int_{-\infty}^{\infty}\int_{-\infty}^{\infty}\delta(t-s)\varphi_j(t)\varphi_k^*(s)\mathrm{d}t\mathrm{d}s \\ &= N_o\int_{-\infty}^{\infty}\varphi_j(t)\varphi_k^*(t)\mathrm{d}t \\ &= N_o\delta_{jk}.\end{aligned}$$

It follows that the $\tilde{n}_k$ are all independent identically distributed zero-mean complex Gaussian random variables with variance N_o. Hence, the vector $\tilde{\mathbf{n}}$ has the multivariate complex Gaussian probability density function (pdf) (A.51)

$$\begin{aligned}p(\tilde{\mathbf{n}}) &= \prod_{i=1}^{N}\frac{1}{2\pi N_o}\exp\left\{-\frac{1}{2N_o}|\tilde{n}_i|^2\right\} \\ &= \frac{1}{(2\pi N_o)^N}\exp\left\{-\frac{1}{2N_o}\|\tilde{\mathbf{n}}\|^2\right\}.\end{aligned} \tag{5.13}$$

The joint pdf $p(\tilde{\mathbf{n}})$ is said to be circularly symmetric, because it appears as a hyperspherical cloud that is centered at the origin in the N-D vector space.

The waveform $\tilde{z}(t)$ is a remainder process due to the fact that $\tilde{z}(t)$ lies outside the vector space that is spanned by the basis functions $\{\varphi_n(t)\}_{n=1}^N$. It is shown below that the remainder process is uncorrelated with received vector $\tilde{\mathbf{r}}$, viz.,

$$\begin{aligned}\frac{1}{2}\mathrm{E}[\tilde{z}(t)r_j^*] &= \frac{1}{2}\mathrm{E}[\tilde{z}(t)]g\tilde{s}_{m_j}^* + \mathrm{E}[\tilde{z}(t)\tilde{n}_j^*] \\ &= \frac{1}{2}\mathrm{E}[\tilde{z}(t)\tilde{n}_j^*] \\ &= \frac{1}{2}\mathrm{E}\left[\left(\tilde{n}(t) - \sum_{n=1}^{N}\tilde{n}_n\varphi_n(t)\right)\tilde{n}_j^*\right] \\ &= \int_{-\infty}^{\infty}\frac{1}{2}\mathrm{E}[\tilde{n}(t)\tilde{n}^*(\tau)]\varphi_j(\tau)\mathrm{d}\tau - \sum_{n=1}^{N}\frac{1}{2}\mathrm{E}[\tilde{n}_n\tilde{n}_j^*]\varphi_n(t) \\ &= N_o\varphi_j(t) - N_o\varphi_j(t) = 0.\end{aligned}$$

[1] Since the $\tilde{n}_k$ have zero mean, their covariances $\lambda_{\tilde{n}_j\tilde{n}_k}$ are equal to their autocorrelations $\phi_{\tilde{n}_j\tilde{n}_k}$. The factor of 1/2 in the definition of the covariance function maintains the conventional usage of N_o as representing the power density spectrum of the low-pass noise process $\tilde{n}(t)$.

Since $\frac{1}{2}\mathrm{E}[\tilde{z}(t)\tilde{r}_j^*] = 0\ ,\ \ j = 1,\ \ldots, N$, it follows that $\tilde{z}(t)$ is uncorrelated with the received vector $\tilde{\mathbf{r}}$. This property implies that the remainder process $\tilde{z}(t)$ is irrelevant when making the decision as to which signal waveform was transmitted, a result known as Wozencraft's irrelevance theorem [357]. In other words, the received vector $\tilde{\mathbf{r}}$ provides "sufficient statistics" for determining which message waveform was transmitted, meaning that $\tilde{\mathbf{r}}$ provides all the necessary information for detection and no other information is required.

5.2 Detection of Known Signals in AWGN

Based on the observation of the noisy received vector $\tilde{\mathbf{r}}$ in (5.11), the receiver should determine which message vector was transmitted such that the probability of decision error is minimized. It is assumed that the receiver has perfect knowledge of the channel gain g. With this in mind, consider the set of a posteriori probabilities

$$\mathrm{P}[\mathbf{s}_i \text{ was sent } |g, \tilde{\mathbf{r}}], \quad i = 1, \ldots, M, \tag{5.14}$$

which is abbreviated as $\mathrm{P}[\mathbf{s}_i|g, \tilde{\mathbf{r}}]$. The maximum a posteriori probability (MAP) receiver decides in favor of the message vector $\tilde{\mathbf{s}}_m$ having the maximum a posteriori probability $\mathrm{P}[\tilde{\mathbf{s}}_m|g, \tilde{\mathbf{r}}]$. That is, the MAP decision rule is

$$\text{choose } \tilde{\mathbf{s}}_m \text{ if } \mathrm{P}[\tilde{\mathbf{s}}_m|g, \tilde{\mathbf{r}}] \geq \mathrm{P}[\tilde{\mathbf{s}}_i|g, \tilde{\mathbf{r}}] \ \ \forall\ i \neq m. \tag{5.15}$$

The probability of error in this decision, denoted by $\mathrm{P}_e[\tilde{\mathbf{s}}_m|g, \tilde{\mathbf{r}}]$, is

$$\begin{aligned} \mathrm{P}_e[\tilde{\mathbf{s}}_m|g, \tilde{\mathbf{r}}] &= \mathrm{P}[\mathbf{s}_m \text{ was not sent } |g, \tilde{\mathbf{r}}] \\ &= 1 - \mathrm{P}[\mathbf{s}_m \text{ was sent } |g, \tilde{\mathbf{r}}] \\ &= 1 - \mathrm{P}[\mathbf{s}_m|g, \tilde{\mathbf{r}}]. \end{aligned} \tag{5.16}$$

Since the MAP receiver always decides in favor of the message vector $\mathbf{s}_m$ having the maximum a posteriori probability $\mathrm{P}[\mathbf{s}_m|g, \tilde{\mathbf{r}}]$ for any received vector $\tilde{\mathbf{r}}$, the probability of error is minimized.

By using Bayes' theorem, the a posteriori probability $\mathrm{P}[\tilde{\mathbf{s}}_m|g, \tilde{\mathbf{r}}]$ can be expressed in the form

$$\mathrm{P}[\tilde{\mathbf{s}}_m|g, \tilde{\mathbf{r}}] = \frac{p(\tilde{\mathbf{r}}|g, \tilde{\mathbf{s}}_m)P_m}{p(\tilde{\mathbf{r}})}\ ,\ \ m = 1,\ \cdots,\ M, \tag{5.17}$$

where $p(\tilde{\mathbf{r}}|g, \tilde{\mathbf{s}}_m)$ is the joint conditional pdf of the received vector $\tilde{\mathbf{r}}$ given the transmitted message vector $\tilde{\mathbf{s}}_m$ and channel gain g, and P_m is the prior probability of transmitting $\tilde{\mathbf{s}}_m$. Since the pdf of the received vector $p(\tilde{\mathbf{r}})$ is independent of the transmitted message vector, the MAP receiver chooses the vector $\tilde{\mathbf{s}}_m$ to maximize $p(\tilde{\mathbf{r}}|g, \tilde{\mathbf{s}}_m)\mathrm{P}_m$. In other words, the MAP decision rule is equivalent to

$$\text{choose } \tilde{\mathbf{s}}_m \text{ if } \quad p(\tilde{\mathbf{r}}|g, \tilde{\mathbf{s}}_m)P_m \geq p(\tilde{\mathbf{r}}|g, \tilde{\mathbf{s}}_i)P_i \ \ \forall\ i \neq m. \tag{5.18}$$

A receiver that chooses the vector $\tilde{\mathbf{s}}_m$ to maximize $p(\tilde{\mathbf{r}}|g, \tilde{\mathbf{s}}_m)$ regardless of the prior messages probabilities is called a maximum likelihood (ML) receiver. The ML decision rule is

$$\text{choose } \tilde{\mathbf{s}}_m \text{ if } \quad p(\tilde{\mathbf{r}}|g, \tilde{\mathbf{s}}_m) \geq p(\tilde{\mathbf{r}}|g, \tilde{\mathbf{s}}_i) \ \ \forall\ i \neq m. \tag{5.19}$$

If the prior message probabilities are all equal, i.e., $P_m = 1/M,\ m = 1,\ \cdots,\ M$, then the signal vector that maximizes $p(\tilde{\mathbf{r}}|g, \tilde{\mathbf{s}}_m)$ also maximizes $p(\tilde{\mathbf{s}}_m|g, \tilde{\mathbf{r}})$. Under this condition the ML receiver minimizes the probability of decision error. In practice, an ML receiver is sometimes implemented regardless of the prior message probabilities, because they may be unknown. Also, the prior message probabilities will be all equal for a well-designed system.

To proceed further, the joint conditional pdf $p(\tilde{\mathbf{r}}|g, \tilde{\mathbf{s}}_m)$ is needed. Since $\tilde{\mathbf{r}} = g\tilde{\mathbf{s}}_m + \tilde{\mathbf{n}}$ and $\tilde{\mathbf{n}}$ has the joint pdf in (5.13), it follows that

$$p(\tilde{\mathbf{r}}|g, \tilde{\mathbf{s}}_m) = \frac{1}{(2\pi N_o)^N} \exp\left\{-\frac{1}{2N_o}\|\tilde{\mathbf{r}} - g\tilde{\mathbf{s}}_m\|^2\right\}. \tag{5.20}$$

By using (5.20) in (5.19), it is apparent that the signal vector $\tilde{\mathbf{s}}_m$ that maximizes $p(\tilde{\mathbf{r}}|g, \tilde{\mathbf{s}}_m)$ also minimizes the exponent in (5.20). Hence, the ML receiver decides in favor of that message $\tilde{\mathbf{s}}_m$ which minimizes the decision metric

$$\mu_1(\tilde{\mathbf{s}}_m) = \|\tilde{\mathbf{r}} - g\tilde{\mathbf{s}}_m\|^2, \quad m = 1, \ldots, M. \tag{5.21}$$

From (5.21), the ML receiver decides in favor of the scaled message vector $g\tilde{\mathbf{s}}_m$ that is closest in squared Euclidean distance (or Euclidean distance) to the received vector $\tilde{\mathbf{r}}$. Such a receiver is said to make minimum distance decisions.

An alternative form of the ML receiver can be derived by first expanding (5.21) as

$$\mu_1(\tilde{\mathbf{s}}_m) = \|\tilde{\mathbf{r}}\|^2 - 2\text{Re}\left\{\tilde{\mathbf{r}} \cdot g^* \tilde{\mathbf{s}}_m^*\right\} + |g|^2 \|\tilde{\mathbf{s}}_m\|^2. \tag{5.22}$$

Then notice that $\|\tilde{\mathbf{r}}\|^2$ is independent of the choice of $\tilde{\mathbf{s}}_m$, and $\|\tilde{\mathbf{s}}_m\|^2 = 2E_m$, where E_m is the energy in the bandpass waveform corresponding to the signal vector $\tilde{\mathbf{s}}_m$. Hence, the ML receiver decides in favor of that message $\tilde{\mathbf{s}}_m$ which maximizes the decision metric

$$\mu_2(\tilde{\mathbf{s}}_m) = \text{Re}\left\{\tilde{\mathbf{r}} \cdot g^* \tilde{\mathbf{s}}_m^*\right\} - |g|^2 E_m \quad , m = 1, \ldots, M. \tag{5.23}$$

Using the definition of the inner product, the above decision metric can be rewritten in the alternate form

$$\begin{aligned} \mu_2(\tilde{\mathbf{s}}_m) &= \text{Re}\left\{\int_{-\infty}^{\infty} \tilde{r}(t) g^* \tilde{s}_m^*(t) \mathrm{d}t\right\} - |g|^2 E_m \\ &\equiv \text{Re}\left\{\int_{-\infty}^{\infty} \tilde{r}(t) \mathrm{e}^{-j\phi} \tilde{s}_m^*(t) \mathrm{d}t\right\} - \alpha E_m \quad , m = 1, \ldots, M. \end{aligned} \tag{5.24}$$

The last line in (5.24) follows because the $\mu_2(\tilde{\mathbf{s}}_m)$ can be divided by α without altering the decision process. In this form of the ML decision metric, the received complex envelope $\tilde{r}(t)$ is correlated directly with the scaled and conjugated signal vector $\mathrm{e}^{-j\phi}\tilde{s}_m^*(t)$.

From the above development, the ML receiver can now be constructed. The receiver must first perform quadrature demodulation as shown in Fig. 5.1 to extract the complex envelope $\tilde{r}(t) = \tilde{r}_I(t) + j\tilde{r}_Q(t)$. The low-pass filter in each branch is used to reject the double frequency term after demodulation. The received bandpass waveform is

$$r(t) = \text{Re}\left\{\tilde{r}(t)\mathrm{e}^{j2\pi f_c t}\right\} = \tilde{r}_I(t)\cos(2\pi f_c t) - \tilde{r}_Q(t)\sin(2\pi f_c t). \tag{5.25}$$

It follows that

$$[r(t) \cdot 2\cos(2\pi f_c t)]_{\text{LP}} = \tilde{r}_I(t) \tag{5.26}$$

$$[-r(t) \cdot 2\sin(2\pi f_c t)]_{\text{LP}} = \tilde{r}_Q(t), \tag{5.27}$$

where $[\,\cdot\,]_{\text{LP}}$ indicates low-pass filtering. After quadrature demodulation, there are several receiver structures that are functionally equivalent, but differ in their method of implementation and complexity. As shown in Fig. 5.2, one possibility is to generate the observation vector $\tilde{\mathbf{r}}$ by correlating the received complex envelope with each of the N basis functions used to define the signal space. This receiver structure is called a correlation detector.

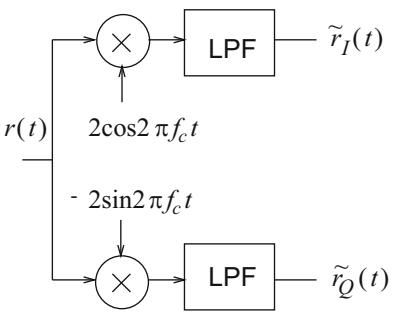

Fig. 5.1 Quadrature demodulator

Fig. 5.2 Correlator detector

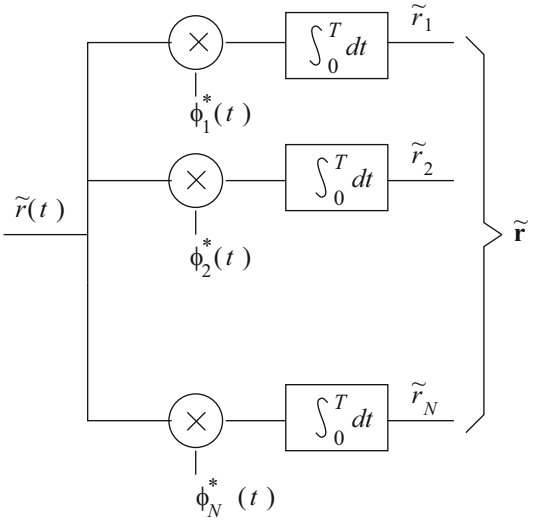

Fig. 5.3 Matched filter detector

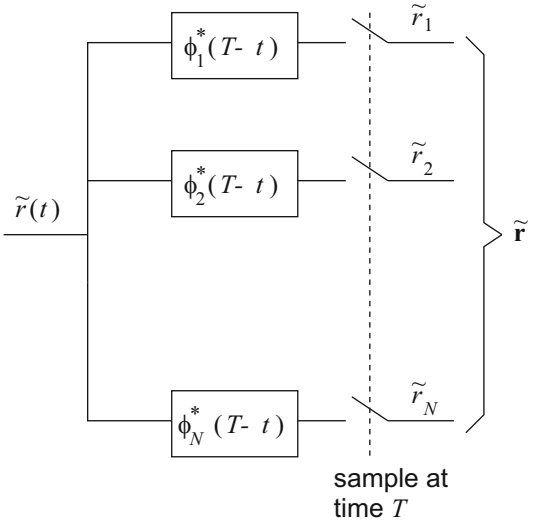

A functionally equivalent structure to the correlation detector is shown in Fig. 5.3, where the complex envelope is filtered with a bank of N filters having impulse responses $\varphi_i^*(T_o - t)$ and sampling the outputs at time T_o, where T_o is the duration of the $\varphi_i(t)$ (or $\tilde{s}_i(t)$). The filter $\varphi_i^*(T_o - t)$ is the *matched filter* to $\varphi_i(t)$ and, therefore, this receiver structure is called a matched filter detector. The matched filter can be shown to be the filter that maximizes the signal-to-noise ratio at the sampling instant when the input consists of a signal corrupted by AWGN (see Problem 5.2). Finally, the metric computer in Fig. 5.4 processes the observation vector $\tilde{\mathbf{r}}$ to produce M decision metrics $\mu_2(\tilde{\mathbf{s}}_m),\ m = 1, \ldots, M$. The decision is made in favor of the message $\tilde{\mathbf{s}}_m$ having the largest decision metric.

To show equivalence of the correlation and matched filter detectors in Figs. 5.2 and 5.3, respectively, let $h_i(t) = \varphi_i^*(T_o - t)$ denote the filter that is matched to $\varphi_i(t)$. Then the output of the matched filter is the convolution

$$\begin{aligned} y(t) &= \int_0^t \tilde{r}(\tau) h_i(t-\tau) \mathrm{d}\tau \\ &= \int_0^t \tilde{r}(\tau) \varphi_i^*(T_o - t + \tau) \mathrm{d}\tau. \end{aligned} \tag{5.28}$$

Sampling the filter output at time T_o gives

$$y(T_o) = \int_0^{T_o} \tilde{r}(\tau) \varphi_i^*(\tau) \mathrm{d}\tau. \tag{5.29}$$

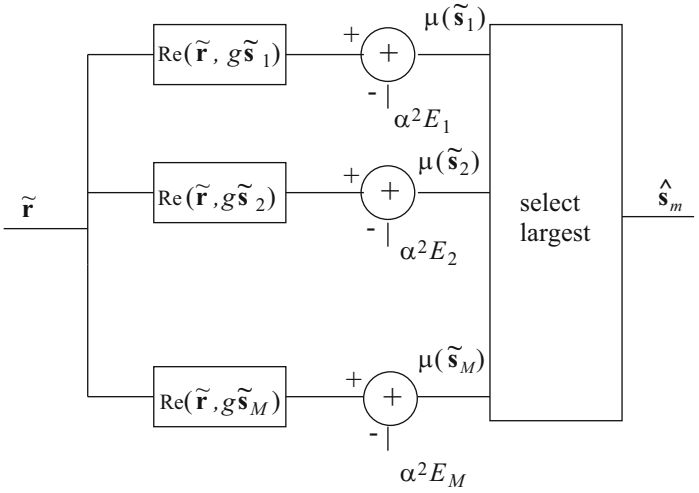

Fig. 5.4 Metric computer

This is exactly the same as the correlation in (5.7). Note that other variations of the ML receiver can be constructed in a similar fashion by direct implementation of (5.24). This will require either a bank of M correlators or a bank of M matched filters, where M is the number of waveforms in the signal set. Since $N \leq M$, the number of correlators or matched filters is usually larger with this latter implementation. However, the outputs of the correlators or matched filters generate the required decision metrics directly, and a subsequent metric computer is not required.

Some simplifications can be made for certain types of signal sets. If the message waveforms have equal energy such as PSK signals, then $E_m = E$ for all m. Hence, the bias term αE_m in (5.23) can be neglected, and the ML receiver decides in favor of that message $\tilde{\mathbf{s}}_m$ which maximizes the decision metric

$$\mu_2(\tilde{\mathbf{s}}_m) = \text{Re}\left\{\tilde{\mathbf{r}} \cdot \mathrm{e}^{-j\phi}\tilde{\mathbf{s}}_m^*\right\} \tag{5.30}$$

$$= \text{Re}\left\{\int_{-\infty}^{\infty} \tilde{r}(t)\mathrm{e}^{-j\phi}\tilde{s}_m^*(t)\mathrm{d}t\right\}, \quad m = 1, \ldots, M. \tag{5.31}$$

In this case, the receiver does not need to know the complete complex channel gain $g = \alpha \mathrm{e}^{j\phi}$, but only the phase ϕ.

5.3 Probability of Error

Consider a signal constellation having the set M signal vectors $\{\tilde{\mathbf{s}}_m\}_{m=1}^M$. Assume that the messages are equally likely so that $P_m = 1/M$. By observing the vector $\tilde{\mathbf{r}}$, the ML receiver chooses that message vector $\tilde{\mathbf{s}}_m$ that minimizes the squared Euclidean distance $\|\tilde{\mathbf{r}} - g\tilde{\mathbf{s}}_m\|^2$. To compute the probability of ML decision error for an arbitrary set of signal vectors, first define convex decision regions R_m around each of the scaled signal vectors $g\tilde{\mathbf{s}}_m$ in the N-D signal space. Figure 5.5 shows an example of the decision regions. Formally, the decision regions are defined by

$$R_m = \left\{\tilde{\mathbf{r}} : \|\tilde{\mathbf{r}} - g\tilde{\mathbf{s}}_m\|^2 \leq \|\tilde{\mathbf{r}} - g\tilde{\mathbf{s}}_i\|^2, \ \forall i \neq m\right\}. \tag{5.32}$$

Observe that every $\tilde{\mathbf{r}} \in R_m$ is closer to $g\tilde{\mathbf{s}}_m$ than to any other scaled signal vector $g\tilde{\mathbf{s}}_i$, $i \neq m$. The ML decision rule becomes

$$\text{choose } \tilde{\mathbf{s}}_m \text{ if } \tilde{\mathbf{r}} \in R_m. \tag{5.33}$$

The decision boundaries are hyperplanes in the N-dimensional signal space that are defined by the locus of signal points that are equidistant from two neighboring scaled signal vectors.

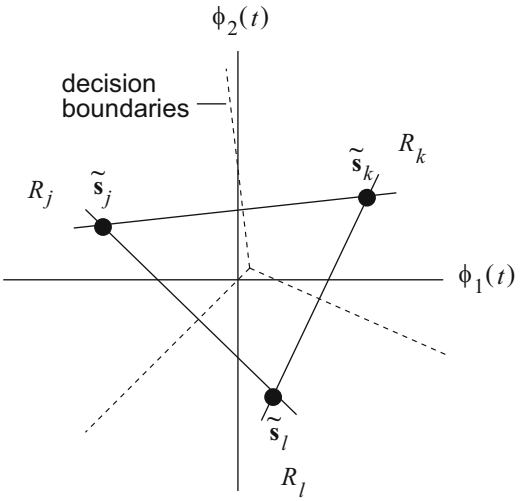

Fig. 5.5 Decision regions in a 2-D signal space

The conditional error probability associated with $\tilde{\mathbf{s}}_m$ is

$$\begin{aligned} \mathrm{P}[e|\tilde{\mathbf{s}}_m] &= \mathrm{P}[\tilde{\mathbf{r}} \notin R_m] \\ &= 1 - \mathrm{P}[\tilde{\mathbf{r}} \in R_m] \\ &= 1 - \mathrm{P}[c|\tilde{\mathbf{s}}_m], \end{aligned} \tag{5.34}$$

where $\mathrm{P}[c|\tilde{\mathbf{s}}_m]$ is the conditional probability of correct reception. By using the joint conditional pdf in (5.20), it follows that

$$\mathrm{P}[e|\tilde{\mathbf{s}}_m] = 1 - \int_{R_m} p(\tilde{\mathbf{r}}|g, \tilde{\mathbf{s}}_m)\mathrm{d}\tilde{\mathbf{r}}. \tag{5.35}$$

Finally, the average probability of decision error is

$$\mathrm{P}[e] = \frac{1}{M}\sum_{m=1}^{M} \mathrm{P}[e|\tilde{\mathbf{s}}_m]. \tag{5.36}$$

It is often difficult if not impossible to compute the exact probability of decision error, due to the difficulty in defining the decision regions R_m and performing the N-fold integration in (5.35) with the proper limits of integration. In this case, various upper and lower bounds, and approximations on the probability of error are useful. First, the concept of pairwise error probability is introduced.

5.3.1 Pairwise Error Probability

Consider two equally likely signal vectors $\tilde{\mathbf{s}}_j$ and $\tilde{\mathbf{s}}_k$ in a signal constellation of size M, as if these two signal vectors are the only ones that exist. The resulting probability of decision error at the receiver is called the pairwise error probability because it can be defined for each distinct pair of signal vectors in the signal constellation. The two signal vectors $\tilde{\mathbf{s}}_j$ and $\tilde{\mathbf{s}}_k$ are separated *at the receiver* by the squared Euclidean distance $\|g\tilde{\mathbf{s}}_j - g\tilde{\mathbf{s}}_k\|^2 = \alpha^2\|\tilde{\mathbf{s}}_j - \tilde{\mathbf{s}}_k\|^2$. A decision boundary can be established at the midpoint between the two signal vectors as shown in Fig. 5.6. Suppose that vector $\tilde{\mathbf{s}}_j$ is sent, and let $\mathrm{P}[e|\tilde{\mathbf{s}}_j]$ denote the probability of ML decision error. This error probability is just the probability that the noise along the vector $g\tilde{\mathbf{s}}_j - g\tilde{\mathbf{s}}_k$ forces the received vector $\tilde{\mathbf{r}} = g\tilde{\mathbf{s}}_j + \tilde{\mathbf{n}}$ to cross the decision boundary. Due to the circularly symmetric property of the AWGN noise, the pdf of the noise vector $\tilde{\mathbf{n}}$ is invariant to its rotation about the origin in the signal space. Hence, the noise component along the line that passes through the two signal vectors will have zero mean and variance N_o. It follows that the error probability is equal to

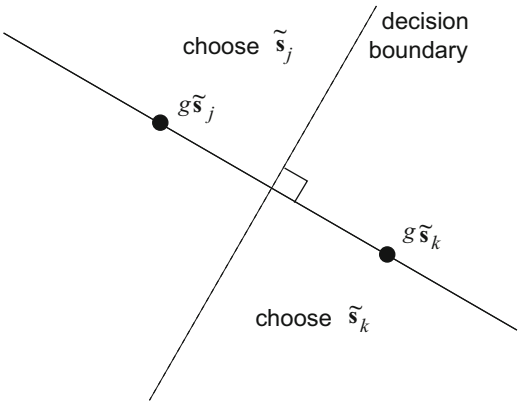

Fig. 5.6 Two received signal points in an N-D signal space

$$\mathrm{P}[e|\tilde{\mathbf{s}}_j] = Q\left(\sqrt{\frac{\alpha^2\tilde{d}_{jk}^2}{4N_o}}\right), \tag{5.37}$$

where $\tilde{d}_{jk}^2 = \|\tilde{\mathbf{s}}_j - \tilde{\mathbf{s}}_k\|^2$ is the squared Euclidean distance between $\tilde{\mathbf{s}}_j$ and $\tilde{\mathbf{s}}_k$. Finally, $\mathrm{P}[e|\tilde{\mathbf{s}}_j] = \mathrm{P}[e|\tilde{\mathbf{s}}_k]$. Hence, the pairwise error probability between the message vectors $\tilde{\mathbf{s}}_j$ and $\tilde{\mathbf{s}}_k$, denoted by $\mathrm{P}[\tilde{\mathbf{s}}_j, \tilde{\mathbf{s}}_k]$, is

$$\mathrm{P}[\tilde{\mathbf{s}}_j, \tilde{\mathbf{s}}_k] = Q\left(\sqrt{\frac{\alpha^2\tilde{d}_{jk}^2}{4N_o}}\right). \tag{5.38}$$

5.3.2 Upper Bounds on Error Probability

Suppose that $\tilde{\mathbf{s}}_k$ is transmitted and let $\mathscr{E}_j$ denote the event that the receiver chooses $\tilde{\mathbf{s}}_j$ instead, thereby making a symbol error. The probability of the event $\mathscr{E}_j$ is the pairwise error probability $\mathrm{P}[\tilde{\mathbf{s}}_j, \tilde{\mathbf{s}}_k]$. The probability of decision error is the probability of the union of all error events

$$\mathrm{P}(e|\tilde{\mathbf{s}}_k) = \mathrm{P}\left[\bigcup_{j\neq k} \mathscr{E}_j\right]. \tag{5.39}$$

Quite often the error events will overlap and this greatly complicates the calculation of the error probability. However, an upper bound on the error probability can be obtained by employing the union bound

$$\mathrm{P}\left[\bigcup_{j\neq k} \mathscr{E}_j\right] \leq \sum_{j\neq k} \mathrm{P}[\mathscr{E}_j]. \tag{5.40}$$

This gives the upper bound

$$\mathrm{P}[e|\tilde{\mathbf{s}}_k] \leq \sum_{j\neq k} \mathrm{P}[\tilde{\mathbf{s}}_j, \tilde{\mathbf{s}}_k]. \tag{5.41}$$

Combining the above result with (5.38) gives

$$\mathrm{P}[e|\tilde{\mathbf{s}}_k] \leq \sum_{j\neq k} Q\left(\sqrt{\frac{\alpha^2\tilde{d}_{jk}^2}{4N_o}}\right) \tag{5.42}$$

and using (5.36) to average error probability over all messages gives

$$\mathrm{P}[e] \le \frac{1}{M}\sum_{k=1}^{M}\sum_{j\neq k} Q\left(\sqrt{\frac{\alpha^2\tilde{d}_{jk}^2}{4N_o}}\right). \tag{5.43}$$

Calculation of the union bound in (5.43) requires the set of squared Euclidean distances $\{\tilde{d}_{jk}^2\}$ between the signal vectors. A simpler upper bound on error probability can be obtained by finding the minimum squared Euclidean distance between any two signal vectors

$$\tilde{d}_{\min}^2 = \min_{n,m} \|\tilde{\mathbf{s}}_n - \tilde{\mathbf{s}}_m\|^2. \tag{5.44}$$

Then the pairwise error probability between $\tilde{\mathbf{s}}_j$ and $\tilde{\mathbf{s}}_k$ is bounded by

$$\mathrm{P}[\tilde{\mathbf{s}}_j, \tilde{\mathbf{s}}_k] \le Q\left(\sqrt{\frac{\alpha^2\tilde{d}_{\min}^2}{4N_o}}\right), \tag{5.45}$$

since $\tilde{d}_{\min}^2 \le \tilde{d}_{jk}^2$ and the function $Q(x)$ monotonically decreases with x. Hence,

$$\mathrm{P}[e] \le (M-1)Q\left(\sqrt{\frac{\alpha^2\tilde{d}_{\min}^2}{4N_o}}\right). \tag{5.46}$$

Finally, some further upper bounds can be obtained by upper bounding the Gaussian Q-function. One such upper bound is (Problem 5.1)

$$Q(x) \le \frac{1}{2}\mathrm{e}^{-x^2/2} \qquad x \ge 0. \tag{5.47}$$

Combining with the union bound in (5.43) gives

$$\mathrm{P}[e] \le \frac{1}{2M}\sum_{k=1}^{M}\sum_{j\neq k} \exp\left\{-\frac{\alpha^2\tilde{d}_{jk}^2}{8N_o}\right\}, \tag{5.48}$$

and combining with the upper bound in (5.46) will give the simplest but loosest upper bound of all

$$\mathrm{P}[e] \le \frac{(M-1)}{2}\exp\left\{-\frac{\alpha^2\tilde{d}_{\min}^2}{8N_o}\right\}. \tag{5.49}$$

5.3.3 *Lower Bound on Error Probability*

A useful lower bound on the probability of decision error can be obtained by bounding the error probability

$$\mathrm{P}[e|\tilde{\mathbf{s}}_k] \ge \begin{cases} Q\left(\sqrt{\frac{\alpha^2\tilde{d}_{\min}^2}{4N_o}}\right), & \text{if } \tilde{\mathbf{s}}_k \text{ has at least one neighbor at distance } \tilde{d}_{\min} \\ 0, & \text{otherwise} \end{cases} \tag{5.50}$$

Then

$$\mathrm{P}[e] = \frac{1}{M}\sum_{m=1}^{M}\mathrm{P}[e|\tilde{\mathbf{s}}_m] \tag{5.51}$$

$$\geq \frac{w_{\min}}{M}Q\left(\sqrt{\frac{\alpha^2\tilde{d}_{\min}^2}{4N_o}}\right), \tag{5.52}$$

where $w_{\min}$ is the number of signal vectors having at least one minimum distance neighbor. Certainly $w_{\min} \geq 2$, so that

$$\mathrm{P}[e] \geq \frac{2}{M}Q\left(\sqrt{\frac{\alpha^2\tilde{d}_{\min}^2}{4N_o}}\right). \tag{5.53}$$

5.3.4 Bit Versus Symbol Error Probabilities

So far, the probability of decision error P[e] otherwise known as the *symbol* error probability, P_M, has been considered. However, the *bit* error probability, P_b, is often of interest. In general, the bit error probability will depend on the particular mapping between the data bits and the modulated symbols. Since each data symbol corresponds to $\log_2 M$ data bits, the bit error probability can be bounded as follows:

$$\frac{P_M}{\log_2 M} \leq P_b \leq P_M. \tag{5.54}$$

The lower bound results from the fact that each symbol error corresponds to at least one bit error, while the upper bound results from the fact that each symbol error corresponds to at most $\log_2 M$ bit errors.

5.3.4.1 Gray Mapping

For signal constellations such as PSK and QAM, it is possible to map the binary data bits onto the data symbols in such a way that the nearest neighboring symbols (in Euclidean distance) differ in only one bit position. Such a mapping is called a Gray mapping. When the signal-to-noise ratio is high, symbol errors tend to be made onto the nearest neighboring symbols with high probability. In these cases, symbol errors correspond to single bit errors. Hence,

$$P_b \approx \frac{P_M}{\log_2 M}. \tag{5.55}$$

It turns out that Gray mapping is the optimum mapping for uncoded systems. However, if error control coding is used, Gray mapping is usually not the optimum mapping strategy and other types of mapping are used. This issue will be discussed in more detail in Chap. 8.

5.3.4.2 Equally Likely Symbol Errors

Suppose that when symbol errors occur, each of the $M-1$ incorrect symbols is chosen with equal probability. To compute the probability of bit error, first note that the set of $M = 2^k$ symbols has a one-to-one mapping onto the set of 2^k binary k-tuples as shown in Fig. 5.7. Now suppose that the all zeroes k-tuple, or first row, corresponds to the correct symbol. Moreover, the receiver makes an error by choosing ith row (symbol), $i \neq 1$, instead. Since there are 2^{k-1} zeros and 2^{k-1} ones in each column, and a zero corresponds to a correct bit, the probability of a particular bit position being in error is

$$P_b = \frac{2^{k-1}}{2^k - 1}P_M = \frac{M}{2(M-1)}P_M. \tag{5.56}$$

It will shown later that this result applies to M-ary orthogonal signals.

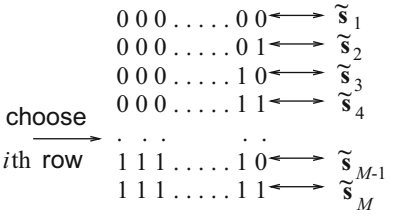

Fig. 5.7 Mapping of binary k-tuples onto M-ary symbols

5.3.5 *Rotation and Translations*

The probability of symbol error in (5.36) is invariant to any rotation of the signal constellation $\{\tilde{\mathbf{s}}_i\}_{i=1}^M$ about the origin of the signal space. This is a consequence of two properties. First, the probability of symbol error depends solely on the set of Euclidean distances $\{\tilde{d}_{jk}\}, j \neq k$ between the signal vectors in the signal constellation. Second, the AWGN is circularly symmetric in all directions of the signal space. A signal constellation can be rotated about the origin of the signal space, by multiplying each N-dimensional signal vector by an $N \times N$ unitary matrix $\mathbf{Q}$. A unitary matrix has the property $\mathbf{Q}\mathbf{Q}^H = \mathbf{Q}^H\mathbf{Q} = I$, where $\mathbf{Q}^H$ is the complex conjugate transpose of $\mathbf{Q}$, and I is the $N \times N$ identity matrix. The rotated signal vectors are equal to

$$\hat{\mathbf{s}}_i = \tilde{\mathbf{s}}_i\mathbf{Q}, \quad i = 1, \ldots, M. \tag{5.57}$$

Correspondingly, the noise vector $\tilde{\mathbf{n}}$ is replaced with its rotated version

$$\hat{\mathbf{n}} = \tilde{\mathbf{n}}\mathbf{Q}. \tag{5.58}$$

The rotated noise vector $\hat{\mathbf{n}}$ is a vector of complex Gaussian random variables that is completely described by its mean and covariance matrix. The mean is

$$\mathrm{E}[\hat{\mathbf{n}}] = \mathrm{E}[\tilde{\mathbf{n}}]\mathbf{Q} = \mathbf{0}. \tag{5.59}$$

The covariance matrix is[2]

$$\begin{aligned}
\mathbf{\Phi}_{\hat{\mathbf{n}}\hat{\mathbf{n}}} &= \frac{1}{2}\mathrm{E}[\hat{\mathbf{n}}^H\hat{\mathbf{n}}] \\
&= \frac{1}{2}\mathrm{E}[(\tilde{\mathbf{n}}\mathbf{Q})^H\tilde{\mathbf{n}}\mathbf{Q}] \\
&= \frac{1}{2}\mathrm{E}[\mathbf{Q}^H\tilde{\mathbf{n}}^H\tilde{\mathbf{n}}\mathbf{Q}] \\
&= \mathbf{Q}^H\frac{1}{2}\mathrm{E}[\tilde{\mathbf{n}}^H\tilde{\mathbf{n}}]\mathbf{Q} \\
&= N_o\mathbf{Q}^H\mathbf{Q} = N_o\mathbf{I}.
\end{aligned} \tag{5.60}$$

Since, the statistical properties of the noise vector are invariant to rotation, the probability of symbol error is invariant to rotation of the signal constellation about the origin of the signal space.

Next consider a translation of the signal set such that

$$\hat{\mathbf{s}}_i = \tilde{\mathbf{s}}_i - \mathbf{a}, \quad i = 1, \ldots, M, \tag{5.61}$$

where $\mathbf{a}$ is a constant vector. In this case, the error probability remains the same since $\hat{d}_{jk} = \tilde{d}_{jk}, j \neq k$. However, the average energy in the signal constellation is altered by the translation and becomes

[2]Since the vector $\hat{\mathbf{n}}$ has zero mean, its covariance matrix $\mathbf{\Lambda}_{\hat{\mathbf{n}}\hat{\mathbf{n}}}$ is equal to its autocorrelation matrix $\mathbf{\Phi}_{\hat{\mathbf{n}}\hat{\mathbf{n}}}$.

$$\begin{aligned}\hat{E}_{\text{av}} &= \frac{1}{2}\sum_{i=1}^{M}\|\hat{\mathbf{s}}_i\|^2 P_i \\ &= \frac{1}{2}\sum_{i=1}^{M}\|\tilde{\mathbf{s}}_i - \mathbf{a}\|^2 P_i \\ &= \frac{1}{2}\sum_{i=1}^{M}\left\{\|\tilde{\mathbf{s}}_i\|^2 - 2\text{Re}\left\{\tilde{\mathbf{s}}_i \cdot \mathbf{a}^*\right\} + \|\mathbf{a}\|^2\right\} P_i \\ &= \frac{1}{2}\sum_{i=1}^{M}\|\tilde{\mathbf{s}}_i\|^2 P_i - \text{Re}\left\{\sum_{i=1}^{M}\tilde{\mathbf{s}}_i P_i \cdot \mathbf{a}^*\right\} + \frac{1}{2}\|\mathbf{a}\|^2\sum_{i=1}^{M} P_i \\ &= E_{\text{av}} - \text{Re}\left\{\text{E}[\,\tilde{\mathbf{s}}\,]\cdot\mathbf{a}^*\right\} + \frac{1}{2}\|\mathbf{a}\|^2 \end{aligned} \tag{5.62}$$

where E_{av} is the average energy of the original signal constellation and $\text{E}[\,\tilde{\mathbf{s}}\,] = \sum_{i=0}^{M-1}\tilde{\mathbf{s}}_i P_i$ is its centroid (or center of mass).

Differentiating (5.62) with respect to $\mathbf{a}$ and setting the result equal to zero will yield the translation that minimizes the average energy in the signal constellation. This gives

$$\mathbf{a}_{\text{opt}} = \text{E}[\,\tilde{\mathbf{s}}\,]. \tag{5.63}$$

Note that the center of mass of the translated signal constellation is at the origin, and the minimum average energy in the translated signal constellation is

$$\hat{E}_{\text{min}} = E_{\text{av}} - \frac{1}{2}\|\mathbf{a}_{\text{opt}}\|^2. \tag{5.64}$$

5.4 Error Probability of PSK

This section considers the error probability of various forms of PSK signals. The treatment starts with binary PSK signals, followed by the more complicated forms of PSK signals.

5.4.1 Error Probability of BPSK

The BPSK signal vectors are[3]

$$\tilde{s}_1 = -\tilde{s}_2 = \sqrt{2E_h}. \tag{5.65}$$

Since there are only two signal vectors, the bit error probability is given by the pairwise error probability in (5.38). For BPSK signals, $\tilde{d}_{12} = 2\sqrt{2E_h}$. Also BPSK transmits 1 bit/symbol so the symbol energy is $E_h = E_b$, where E_b is the bit energy. Therefore, the probability of bit error is

$$P_b(\gamma_b) = Q\left(\sqrt{2\gamma_b}\right) \tag{5.66}$$

where γ_b is defined as the received *bit energy-to-noise ratio*

$$\gamma_b \triangleq \frac{\alpha^2 E_b}{N_o}. \tag{5.67}$$

[3]When the signal vectors lie in a 1-D complex vector space, the notation is simplified by using the scalars $\tilde{s}_i$, $\tilde{n}$, $\tilde{r}$ rather than the vectors $\tilde{\mathbf{s}}_i$, $\tilde{\mathbf{n}}$, and $\tilde{\mathbf{r}}$.

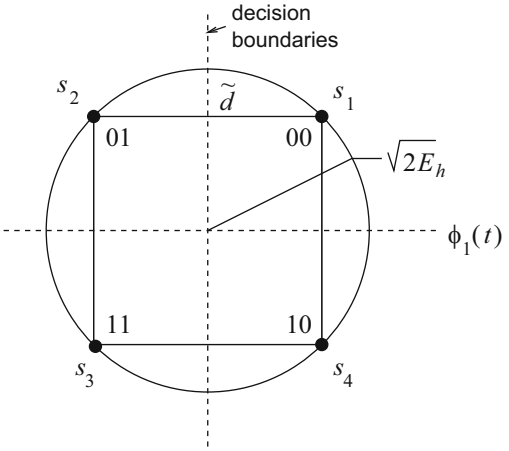

Fig. 5.8 Complex signal-space diagram for QPSK

5.4.2 *Error Probability of QPSK and OQPSK*

The QPSK (or 4-PSK) signal vectors are

$$\tilde{s}_1 = -\tilde{s}_3 = \sqrt{2E_h} \tag{5.68}$$

$$\tilde{s}_2 = -\tilde{s}_4 = j\sqrt{2E_h}, \tag{5.69}$$

where the signal points are seen to lie on the real and imaginary axes. The QPSK signal constellation can be rotated by 45° as shown in Fig. 5.8 without changing the error probability due to the rotational invariance property. In this case, the decision boundaries correspond to the real and imaginary axes of the complex signal space. The noise vector is $\tilde{n} = \tilde{n}_I + j\tilde{n}_Q$, where $\tilde{n}_I$ and $\tilde{n}_Q$ are independent zero-mean Gaussian random variables with variance N_o. With minimum distance decisions, the probability of symbol error is

$$\begin{aligned} P_M &= \mathrm{P}[e|\tilde{s}_1] \\ &= 1 - \mathrm{P}[c|\tilde{s}_1] \\ &= 1 - \mathrm{P}\left[\tilde{n}_I > -\alpha\tilde{d}/2, \tilde{n}_Q > -\alpha\tilde{d}/2\right] \\ &= 1 - \mathrm{P}\left[\tilde{n}_I > -\alpha\tilde{d}/2\right]\mathrm{P}\left[\tilde{n}_Q > -\alpha\tilde{d}/2\right] \\ &= 1 - \left(1 - Q\left(\sqrt{\frac{\alpha^2\tilde{d}^2}{4N_o}}\right)\right)^2 \end{aligned}$$

where, again, α is the channel attenuation. Since $\tilde{d}^2 = 4E_h$,

$$P_M = 1 - \left(1 - Q\left(\sqrt{\gamma_s}\right)\right)^2 \tag{5.70}$$

where γ_s is defined as the received *symbol energy-to-noise ratio*

$$\gamma_s \triangleq \frac{\alpha^2 E_h}{N_o}. \tag{5.71}$$

Suppose the data bits are mapped onto the data symbols with the Gray code shown in Fig. 5.8. Letting P_b denote the probability of bit error, it follows that

$$\mathrm{P}[c] = (1 - P_b)^2 \tag{5.72}$$

and

$$P_M = 1 - (1 - P_b)^2. \tag{5.73}$$

Comparing (5.73) with (5.70), observe that

$$P_b = Q\left(\sqrt{\gamma_s}\right). \tag{5.74}$$

QPSK transmits 2 bits/symbol so the symbol energy is $E_h = 2E_b$, where E_b is the bit energy. Since $\gamma_s = 2\gamma_b$, the probability of bit error is

$$P_b(\gamma_b) = Q\left(\sqrt{2\gamma_b}\right). \tag{5.75}$$

Notice that the bit error rate performances of QPSK and BPSK are identical. Finally, since OQPSK is identical to QPSK with the exception that the in-phase and quadrature branches are offset by $T_b = T/2$ seconds, the bit error rate performance of OQPSK is identical to that of QPSK and BPSK as well.

5.4.3 *Error Probability of M-PSK*

To derive the error probability of M-PSK consider, for example, the 8-PSK signal constellation and associated decision regions shown in Fig. 5.9. Once again data bits are mapped onto data symbols by using a Gray code. Suppose that the message vector $\tilde{s}_1 = \sqrt{2E_h}$ is transmitted. The received signal vector is

$$\tilde{r} = \alpha e^{j\phi}\tilde{s}_1 + \tilde{n}. \tag{5.76}$$

Since the error probability is invariant to the angle rotation ϕ, it is possible to arbitrarily set $\phi = 0$ so that

$$\begin{aligned} \tilde{r} &= \alpha\tilde{s}_1 + \tilde{n} \\ &= \alpha\sqrt{2E_h} + \tilde{n}. \end{aligned} \tag{5.77}$$

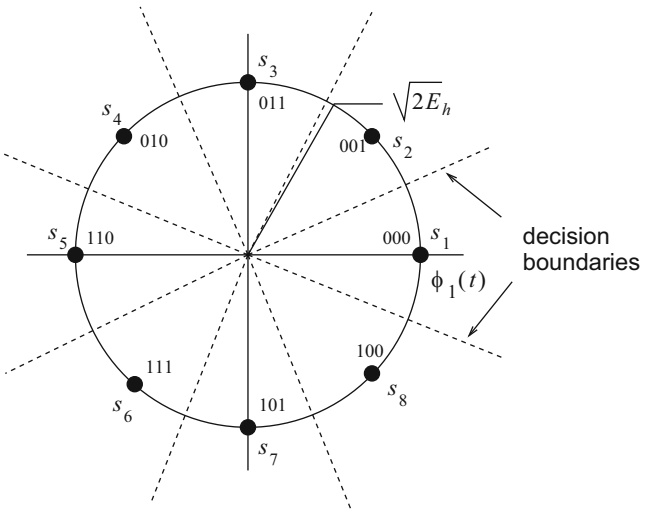

Fig. 5.9 Complex signal-space diagram for 8-PSK along with the associated decision regions

It follows that $\tilde{r} = \tilde{r}_I + j\tilde{r}_Q$ is a complex Gaussian random variable with pdf

$$p_{\tilde{r}}(\tilde{r}) = \frac{1}{\pi N_o} \exp\left\{-\frac{1}{N_o}\left|\tilde{r} - \alpha\sqrt{2E_h}\right|^2\right\}. \tag{5.78}$$

Since $\tilde{s}_1$ was transmitted, the probability of correct symbol reception with minimum distance decisions is the probability that the received vector $\tilde{r}$ falls in the "pie-shaped" region containing $\tilde{s}_1$. This is equivalent to the received angle $\Theta = \text{Tan}^{-1}[\tilde{r}_Q/\tilde{r}_I]$ falling in the interval $[-\pi/8, \pi/8]$.

To find the pdf of the angle Θ, first define the random variables

$$R = \sqrt{\tilde{r}_I^2 + \tilde{r}_Q^2}\,, \qquad \Theta = \text{Tan}^{-1}\left[\tilde{r}_Q/\tilde{r}_I\right] \tag{5.79}$$

such that

$$\tilde{r}_I = R\cos\Theta\,, \qquad \tilde{r}_Q = R\sin\Theta. \tag{5.80}$$

Then by using a bivariate transformation of random variables as shown in Appendix A, the joint pdf of R and Θ can be obtained as

$$p_{R,\Theta}(r,\theta) = \frac{r}{\pi N_o} e^{-\frac{1}{N_o}\left(r^2 - 2\alpha\sqrt{2E_h}r\cos\theta + 2\alpha^2E_h^2\right)}, \quad r \geq 0, -\pi \leq \theta \leq \pi. \tag{5.81}$$

Since only the phase Θ is of interest, the marginal pdf of Θ is obtained as

$$p_\Theta(\theta) = \int_0^\infty p_{R,\Theta}(r,\theta)\mathrm{d}r \tag{5.82}$$

$$= \frac{1}{2\pi} e^{-\gamma_s \sin^2\theta} \int_0^\infty x e^{\left(x - \sqrt{2\gamma_s}\cos\theta\right)^2/2}\mathrm{d}x, \tag{5.83}$$

where $\gamma_s = \alpha^2 E_h/N_o$ is the received symbol energy-to-noise ratio. The probability of symbol error, P_M, is just the probability that Θ falls outside the region $[-\pi/M, \pi/M]$. Thus

$$P_M(\gamma_s) = 1 - \int_{-\pi/M}^{\pi/M} p(\theta)\mathrm{d}\theta. \tag{5.84}$$

Unfortunately, a closed form expression for this integral does not exist, except for the cases $M = 2, 4$ which were considered earlier.

5.4.4 Error Probability with Rayleigh Fading

When the channel experiences fading, the error probability must be averaged over the fading distribution. For example, if the channel is Rayleigh faded, then α is a Rayleigh random variable and the squared-envelope α^2 is an exponential random variable at any given time, as discussed in Sect. 2.1.3.1. It follows that the received bit and symbol-energy-to-noise ratios γ_b and γ_s in (5.67) and (5.71), respectively, have the exponential pdfs

$$p_{\gamma_b}(x) = \frac{1}{\bar{\gamma}_b} e^{-x/\bar{\gamma}_b}\,, \quad x \geq 0 \tag{5.85}$$

and

$$p_{\gamma_s}(x) = \frac{1}{\bar{\gamma}_s} e^{-x/\bar{\gamma}_s}\,, \quad x \geq 0, \tag{5.86}$$

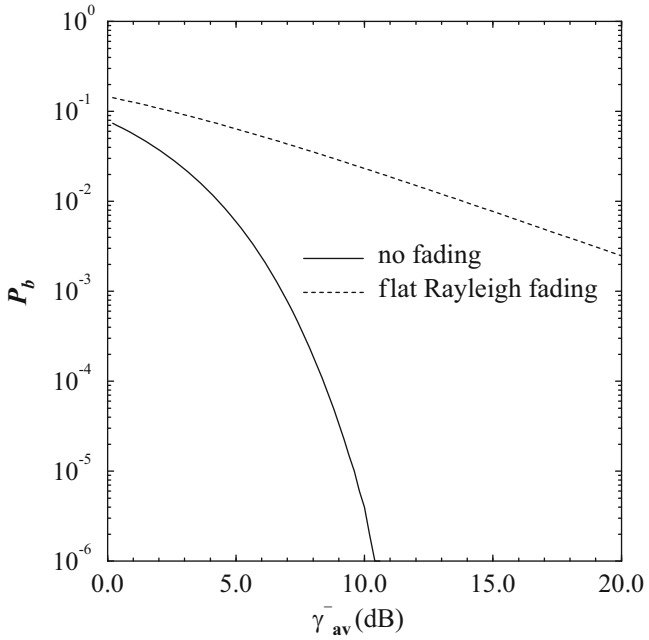

Fig. 5.10 Bit error probability for BPSK and QPSK for a slow flat Rayleigh fading channel with AWGN

where $\bar{\gamma}_b$ and $\bar{\gamma}_s$ are the average received bit and symbol energy-to-noise ratios, respectively. Since there are $\log_2 M$ bits per modulated symbol, it also follows that $\gamma_s = \gamma_b \log_2 M$ and $\bar{\gamma}_s = \bar{\gamma}_b \log_2 M$. Corresponding expressions for the distribution of γ_b and γ_s can be obtained in a similar fashion for other types of fading, such as Ricean and Nakagami fading.

For BPSK and QPSK, the probability of bit error averaged over the distribution of the received bit energy-to-noise ratio in (5.85) is

$$\begin{aligned} P_b &= \int_0^\infty Q(\sqrt{2x}) p_{\gamma_b}(x) \mathrm{d}x \\ &= \frac{1}{2}\left(1 - \sqrt{\frac{\bar{\gamma}_b}{1+\bar{\gamma}_b}}\right) \\ &\approx \frac{1}{4\bar{\gamma}_b} \qquad \text{for } \bar{\gamma}_b \gg 1. \end{aligned} \tag{5.87}$$

The BPSK and QPSK bit error probability is plotted in Fig. 5.10 for an AWGN channel and a Rayleigh fading channel. Observe that Rayleigh fading converts an exponential dependency of the bit error probability on the average received bit energy-to-noise ratio into an inverse linear one. This behavior with flat Rayleigh fading will be observed for all types of modulation, and it results in a huge loss in performance unless appropriate countermeasures such as diversity and coding are used. For M-PSK, the average symbol error probability is

$$P_M = \int_0^\infty P_M(x) p_{\gamma_s}(x) \mathrm{d}x \tag{5.88}$$

where $P_M(x)$ is given by (5.84) and γ_s is given by (5.86). Although no closed form expression exists, numerical results will show that the bit error probability depends inversely on the average received bit energy-to-noise ratio $\bar{\gamma}_b$. Recall that with Gray coding the bit error probability is approximately $P_b \approx P_M / \log_2 M$.

5.4.5 Differential PSK

The received carrier phase for PSK signals is

$$\theta_k = \frac{2\pi}{M} x_k + \phi, \tag{5.89}$$

where ϕ is the random phase due to the channel. The receiver corrects for the phase ϕ by multiplying the received complex envelope by $e^{-j\phi}$ as shown in (5.31). However, in practice this operation is not quite that simple, because the symmetries in the signal constellation create *phase ambiguity*. In particular, any channel induced phase of the form $\phi + 2k\pi/M$, where k an integer, will lead to exactly the same set of received carrier phases. While the receiver can use a phased locked loop to recover the received carrier phase, there will remain a phase ambiguity which is a multiple of $2\pi/M$. This phase ambiguity must be resolved if the information is to be recovered correctly.

Differential encoding is one of the most popular methods for resolving phase ambiguity, where information is transmitted in the carrier phase differences between successive baud intervals rather than the absolute carrier phases. Differential encoding of PSK signals is done as follows. The information sequence $\{x_k\}, x_k \in \{0, 1, \ldots M-1\}$ is differentially encoded into a new sequence $\{d_k\}$ according to

$$d_k = x_k \oplus x_{k-1}, \tag{5.90}$$

where $\oplus$ denotes modulo-M addition. Then the sequence $\{d_k\}$ is transmitted in the absolute carrier phase according to

$$\theta_k = \frac{2\pi}{M} d_k. \tag{5.91}$$

After carrier recovery, the received carrier phase is

$$\tilde{\theta}_k = \frac{2\pi}{M} d_k + \frac{2\pi\ell}{M}, \tag{5.92}$$

where the additional term $2\pi\ell/M$, ℓ an integer, represents the phase ambiguity. The receiver computes the differential phase

$$\begin{aligned} \tilde{\theta}_k - \tilde{\theta}_{k-1} \text{ modulo } 2\pi &= \frac{2\pi}{M}(d_k - d_{k-1}) \text{ modulo } 2\pi \\ &= \frac{2\pi}{M}(d_k \ominus d_{k-1}) \\ &= \frac{2\pi}{M} x_k \end{aligned} \tag{5.93}$$

where $\ominus$ denotes modulo-M subtraction. Hence, the data sequence $\{x_k\}$ can be recovered regardless of the phase ambiguity.

In the presence of AWGN noise, the receiver must form estimates $\hat{\theta}_k$ of the received carrier phases $\tilde{\theta}_k$. However, the noise will cause errors in these estimates and occasionally $\hat{\theta}_k \neq \tilde{\theta}_k$. Note that an incorrect phase estimate $\hat{\theta}_k$ causes the decisions for both x_k and x_{k-1} to be in error, assuming that the phase estimates $\hat{\theta}_{k-1}$ and $\hat{\theta}_{k+1}$ are both correct. Hence, at high signal-to-noise ratios where errors occur infrequently, the bit error probability of Differential PSK (DPSK) is roughly two times that of PSK.

5.5 Error Probability of PAM and QAM

5.5.1 Error Probability of M-PAM

Consider the Gray coded 8-PAM system signal constellation shown in Fig. 5.11. For the $M-2$ inner points of the signal constellation, the probability of symbol error is

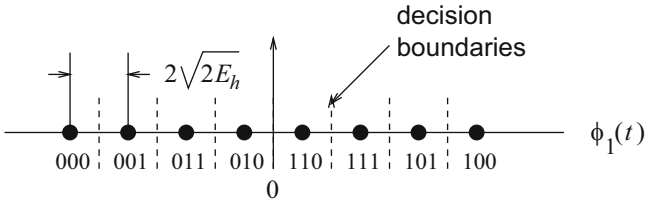

Fig. 5.11 Complex signal-space diagram for 8-PAM

$$P_i = 2Q\left(\frac{2\alpha^2 E_h}{N_o}\right). \tag{5.94}$$

Likewise, for the 2 outer points of the signal constellation, the probability of symbol error is

$$P_o = Q\left(\sqrt{\frac{2\alpha^2 E_h}{N_o}}\right). \tag{5.95}$$

Assuming all points in the signal constellation are used with equal probability, the overall probability of symbol error is

$$\begin{aligned} P_M &= \frac{M-2}{M}P_i + \frac{2}{M}P_o \\ &= 2\left(1-\frac{1}{M}\right)Q\left(\sqrt{\frac{2\alpha^2 E_h}{N_o}}\right). \end{aligned} \tag{5.96}$$

To proceed further, E_h must be related to the average symbol energy. Since

$$\tilde{s}_m = \sqrt{2E_h}(2m-1-M)\,, \quad m = 1,\ldots,M \tag{5.97}$$

the energy in $\tilde{s}_m$ is

$$E_m = \frac{1}{2}\tilde{s}_m^2 = E_h(2m-1-M)^2. \tag{5.98}$$

The average energy is

$$\begin{aligned} E_{\text{av}} &= E_h\frac{1}{M}\sum_{m=1}^{M}(2m-1-M)^2 \\ &= E_h\frac{1}{M}\left(4\sum_{m=1}^{M}m^2 - 4(M+1)\sum_{m=1}^{M}m + M(M+1)^2\right). \end{aligned} \tag{5.99}$$

Using the identities

$$\sum_{k=1}^{n}k = \frac{n(n+1)}{2}\,, \qquad \sum_{k=1}^{n}k^2 = \frac{n(n+1)(2n+1)}{6} \tag{5.100}$$

and simplifying gives the result

$$E_{\text{av}} = E_h\frac{M^2-1}{3}. \tag{5.101}$$

Hence, from (5.96)

$$P_M(\gamma_s) = 2\left(1 - \frac{1}{M}\right) Q\left(\sqrt{\frac{6}{M^2 - 1}\gamma_s}\right), \tag{5.102}$$

where

$$\gamma_s = \frac{\alpha^2 E_{\text{av}}}{N_o} \tag{5.103}$$

is the average symbol energy-to-noise ratio. Note that in this case, the "average" is over the points in the signal constellation. Since $\gamma_s = (\log_2 M)\gamma_b$,

$$P_M(\gamma_b) = 2\left(1 - \frac{1}{M}\right) Q\left(\sqrt{\frac{6(\log_2 M)}{M^2 - 1}\gamma_b}\right). \tag{5.104}$$

5.5.2 *Error Probability of M-QAM*

Consider an M-QAM system having a square constellation of size $M = 4^m$ for some integer m. Such an M-QAM system can be viewed as two $\sqrt{M}$-PAM systems in quadrature, each allocated one-half the power of the M-QAM system. For example, the Gray coded 16-QAM system in Fig. 5.12 can be treated as two independent Gray coded 4-PAM systems in quadrature, each operating with half the power of the 16-QAM system. From (5.102), the symbol error probability for each $\sqrt{M}$-PAM system is

$$P_{\sqrt{M}} = 2\left(1 - \frac{1}{\sqrt{M}}\right) Q\left(\sqrt{\frac{6}{M - 1}\frac{\gamma_s}{2}}\right), \tag{5.105}$$

where γ_s is the average symbol energy-to-noise ratio of the M-QAM system. Finally, the probability of correct symbol reception in the M-QAM system is

$$\mathrm{P}[c] = (1 - P_{\sqrt{M}})^2 \tag{5.106}$$

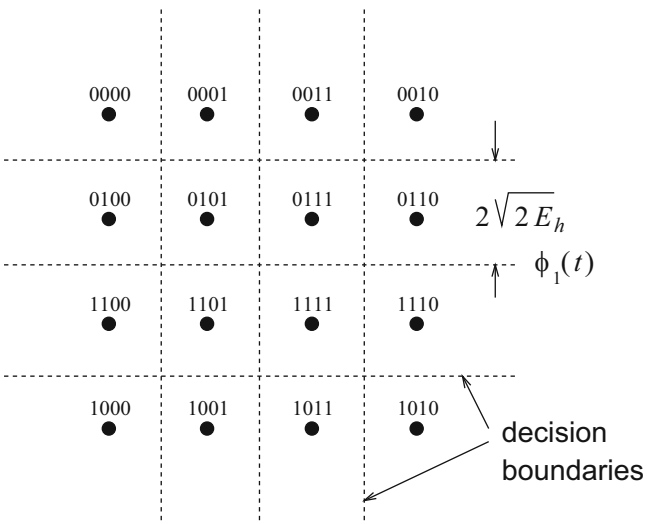

Fig. 5.12 Complex signal-space diagram for 16-QAM constellation

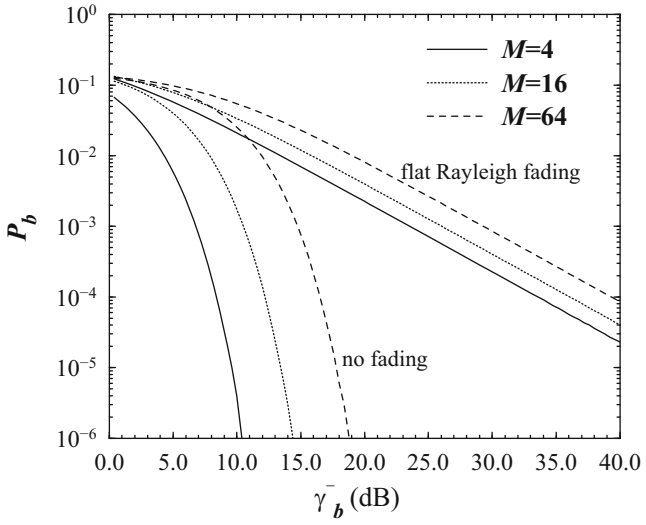

Fig. 5.13 Bit error probability for M-QAM on an AWGN channel and a Rayleigh fading channel with AWGN

and the probability of symbol error is

$$P_M(\gamma_s) = 1 - (1 - P_{\sqrt{M}})^2. \tag{5.107}$$

For other types of M-QAM constellations, such as those in Figs. 4.7 and 4.8, the error probability can be obtained by defining convex decision regions and using the approach suggested in Sect. 5.3.

5.5.2.1 Error Probability with Rayleigh Fading

If the channel is Rayleigh faded, then γ_s has the exponential pdf in (5.86). It follows that the average symbol error probability is

$$P_M = \int_0^\infty P_M(x) p_{\gamma_s}(x) \mathrm{d}x. \tag{5.108}$$

Figure 5.13 plots the (approximate) bit error probability $P_b \approx P_M/\log_2 M$ against the average received *bit* energy-to-noise ratio, $\bar{\gamma}_b = \bar{\gamma}_s/\log_2 M$, for several values of M. Once again, Rayleigh fading converts an exponential dependency of the bit error probability on the average received bit energy-to-noise ratio into an inverse linear one. Finally, notice that the $\bar{\gamma}_b$ required to achieve a given bit error probability increases with the alphabet size M. However, the bandwidth efficiency also increases with M, since there are $\log_2 M$ bits per modulated symbol.

5.6 Error Probability of Orthogonal Signals

5.6.1 Orthogonal Signals

Consider the M-ary orthogonal signal set

$$\tilde{\mathbf{s}}_i = \sqrt{2E_h}\mathbf{e}_m, \quad m = 1, \ldots, M,$$

where $\mathbf{e}_m$ is a length-M unit basis vector with a "1" in the mth coordinate. If the signal $\tilde{\mathbf{s}}_1$ is transmitted, then the received vector is

$$\tilde{\mathbf{r}} = (g\sqrt{2E_h} + \tilde{n}_1, \tilde{n}_2, \ldots, \tilde{n}_M), \tag{5.109}$$

where the $\tilde{n}_i$ are independent zero-mean complex Gaussian random variables with variance N_o. The ML receiver computes the M decision variables

$$\mu(\tilde{\mathbf{s}}_m) = \mathrm{Re}\left\{\tilde{\mathbf{r}} \cdot g^* \tilde{\mathbf{s}}_m^*\right\}, \quad m = 1, \ldots, M, \tag{5.110}$$

and decides in favor of the signal having the largest $\mu(\tilde{\mathbf{s}}_m)$. It follows that

$$\begin{aligned} \mu(\tilde{\mathbf{s}}_1) &= 2\alpha^2 E_h + \tilde{n}_{I,1}\alpha\sqrt{2E_h} \\ \mu(\tilde{\mathbf{s}}_m) &= \tilde{n}_{I,m}\alpha\sqrt{2E_h}, \quad m = 2, \ldots, M, \end{aligned} \tag{5.111}$$

where the phase rotation on the noise samples has been ignored due to their circular symmetry. The $\mu(\tilde{\mathbf{s}}_i), i = 1, \ldots, M$, are independent Gaussian random variables with variance $2\alpha^2 E N_o$; the mean of $\mu(\tilde{\mathbf{s}}_1)$ is $2\alpha^2 E_h$ while the $\mu(\tilde{\mathbf{s}}_m), m \neq 1$, have zero mean. The probability of correct symbol decision conditioned on $\mu(\tilde{\mathbf{s}}_1) = x$ is the probability that all the $\mu(\tilde{\mathbf{s}}_m), m \neq 1$ are less than x. This is just

$$P[c|\mu(\tilde{\mathbf{s}}_0) = x] = \left(\Phi\left(\frac{x}{\sqrt{2\alpha^2 E_h N_o}}\right)\right)^{M-1}. \tag{5.112}$$

Hence,

$$P[c] = \int_{-\infty}^{\infty} \left(\Phi\left(\frac{x}{\sqrt{2\alpha^2 E_h N_o}}\right)\right)^{M-1} \frac{1}{\sqrt{4\pi\alpha^2 E_h N_o}} \exp\left\{-\frac{(x - 2\alpha^2 E_h)^2}{4\alpha^2 E_h N_o}\right\} \mathrm{d}x. \tag{5.113}$$

Now let $y = (x - 2\alpha^2 E_h)/\sqrt{2\alpha^2 E_h N_o}$. Then

$$P[c] = \int_{-\infty}^{\infty} \left(\Phi\left(y + \sqrt{2\gamma_s}\right)\right)^{M-1} \frac{1}{\sqrt{2\pi}} \mathrm{e}^{-y^2/2} \mathrm{d}x, \tag{5.114}$$

where

$$\gamma_s = \frac{\alpha^2 E_h}{N_o}. \tag{5.115}$$

Finally, the probability of symbol error is

$$P_M = 1 - P[c]. \tag{5.116}$$

An alternate expression for the error probability can be derived by first conditioning on the event that one of the $M - 1$ decision variables $\mu(\tilde{\mathbf{s}}_m), m \neq 1$ is the largest. This gives

$$P_M = (M-1)\int_{-\infty}^{\infty} \Phi\left(\frac{x - 2\alpha^2 E_h}{\sqrt{2\alpha^2 E_h N_o}}\right) \left(\Phi\left(\frac{x}{\sqrt{2\alpha^2 E_h N_o}}\right)\right)^{M-2} \frac{1}{\sqrt{4\pi\alpha^2 E_h N_o}} \exp\left\{-\frac{x^2}{4\alpha^2 E_h N_o}\right\} \mathrm{d}x. \tag{5.117}$$

Now let $y = x/\sqrt{2\alpha^2 E_h N_o}$. Then

$$P_M = (M-1)\int_{-\infty}^{\infty} \Phi\left(y - \sqrt{2\gamma_s}\right) (\Phi(y))^{M-2} \frac{1}{\sqrt{2\pi}} \mathrm{e}^{-y^2/2} \mathrm{d}x. \tag{5.118}$$

For orthogonal signals $\gamma_s = \gamma_b \log_2 M$ and the bit error probability is given by (5.56). Hence,

$$P_b = \frac{M}{2} \int_{-\infty}^{\infty} \Phi\left(y - \sqrt{2\gamma_b \log_2 M}\right) (\Phi(y))^{M-2} \frac{1}{\sqrt{2\pi}} \mathrm{e}^{-y^2/2} \mathrm{d}x. \tag{5.119}$$

If the channel is Rayleigh faded, then γ_b has the exponential pdf in (5.85), and the average bit error probability can be calculated as

$$P_b = \int_0^{\infty} P_b(x) p_{\gamma_b}(x) \mathrm{d}x. \tag{5.120}$$

5.6.2 *Biorthogonal Signals*

Consider the biorthogonal signal set

$$\tilde{\mathbf{s}}_i = \begin{cases} \sqrt{2E_h}\mathbf{e}_i\,, & i = 1, \ldots, M/2 \\ -\tilde{\mathbf{s}}_{i-M/2}\,, & i = M/2+1, \ldots, M-1 \end{cases}. \tag{5.121}$$

Now suppose that $\mathbf{s}_1$ is transmitted. The receiver computes the $M/2$ decision variables

$$\mu(\tilde{\mathbf{s}}_m) = \mathrm{Re}\left\{\tilde{\mathbf{r}} \cdot g^* \tilde{\mathbf{s}}_m^*\right\}\,, \quad m = 1, \ldots, M/2, \tag{5.122}$$

and chooses the one having the largest magnitude. The sign of $\mu(\tilde{\mathbf{s}}_m)$ is used to decide whether $\tilde{\mathbf{s}}_m$ or $\tilde{\mathbf{s}}_{M/2+m} = -\tilde{\mathbf{s}}_m$ was sent. As before, the $\mu(\tilde{\mathbf{s}}_i),\ i = 1, \ldots, M/2$, are independent Gaussian random variables with variance $2\alpha^2 E N_o$; the mean of $\mu(\tilde{\mathbf{s}}_1)$ is $2\alpha^2 E_h$ while the $\mu(\tilde{\mathbf{s}}_m), m = 2, \ldots, M/2$, have zero mean. The probability of correct decision is the probability that $\mu(\tilde{\mathbf{s}}_1) > 0$ and $|\mu(\tilde{\mathbf{s}}_m)| < \mu(\tilde{\mathbf{s}}_1), m = 2, \ldots, M/2$. Conditioned on $\mu(\tilde{\mathbf{s}}_1) = x, x > 0$,

$$P\left[|\mu(\tilde{\mathbf{s}}_m)| < x\right] = \Phi\left(\frac{x}{\sqrt{2\alpha^2 E_h N_o}}\right) - \Phi\left(-\frac{x}{\sqrt{2\alpha^2 E_h N_o}}\right). \tag{5.123}$$

Hence,

$$P[c] = \int_0^{\infty} \left(\Phi\left(\frac{x}{\sqrt{2\alpha^2 E_h N_o}}\right) - \Phi\left(-\frac{x}{\sqrt{2\alpha^2 E_h N_o}}\right)\right)^{M/2-1} \frac{1}{\sqrt{4\pi\alpha^2 E_h N_o}} \exp\left\{-\frac{(x - 2\alpha^2 E_h)^2}{4\alpha^2 E_h N_o}\right\} \mathrm{d}x. \tag{5.124}$$

Now let $y = (x - 2\alpha^2 E_h)/\sqrt{2\alpha^2 E_h N_o}$. Then

$$P[c] = \int_{-\sqrt{2\gamma_s}}^{\infty} \left(\Phi\left(y + \sqrt{2\gamma_s}\right) - \Phi\left(-y - \sqrt{2\gamma_s}\right)\right)^{M/2-1} \frac{1}{\sqrt{2\pi}} \mathrm{e}^{-y^2/2} \mathrm{d}y. \tag{5.125}$$

Finally, $P_M = 1 - P[c]$. For biorthogonal signals $\gamma_s = \gamma_b \log_2 M$. However, the bit error probability is not given by (5.56), because when symbol errors occur the incorrect symbols do not occur with equal probability.

5.7 Error Probability of OFDM

The OFDM baseband demodulator is usually implemented by using a fast Fourier transform (FFT), as discussed in Sect. 4.6. Following the development in Sect. 4.6, suppose that the discrete-time sequence $\mathbf{X}_n^g = \{X_{n,m}^g\}_{m=0}^{N+G-1}$ is passed through a balanced pair of digital-to-analog converters (DACs), as shown in Fig. 4.14, and the resulting complex envelope is transmitted over a quasi-static flat fading channel with complex gain g. The quasi-static assumption means that the channel remains static over an OFDM symbol, but can vary from one OFDM symbol to the next. For flat fading channels, the cyclic guard interval

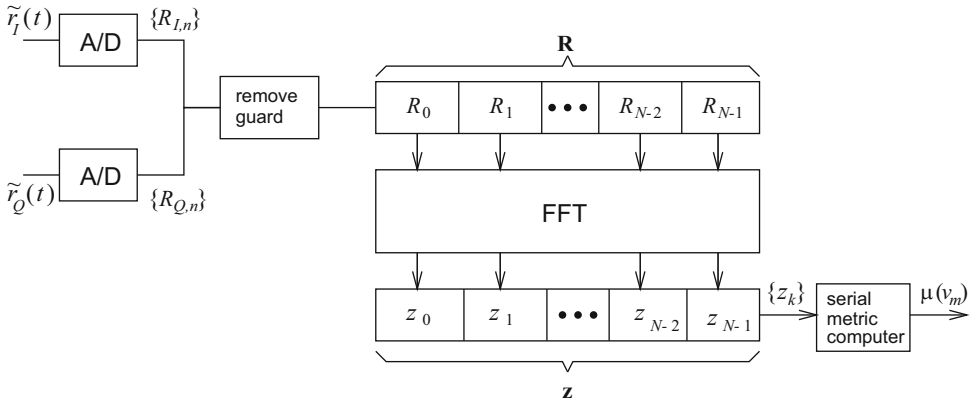

Fig. 5.14 Block diagram of OFDM receiver

is not really necessary, but is included here for simplicity. The receiver uses a quadrature demodulator to extract the received complex envelope $\tilde{r}(t) = \tilde{r}_I(t) + j\tilde{r}_Q(t)$. Suppose that the quadrature components $\tilde{r}_I(t)$ and $\tilde{r}_Q(t)$ are each passed through an ideal anti-aliasing filter (ideal low-pass filter) having a cutoff frequency $1/(2T_s^g)$ followed by an analog-to-digital converter (ADC) as shown in Fig. 5.14. This produces the received complex-valued sample sequence $\mathbf{R}_n^g = \{R_{n,m}^g\}_{m=0}^{N+G-1}$, where

$$R_{n,m}^g = gX_{n,m}^g + \tilde{n}_{n,m}, \tag{5.126}$$

$g = \alpha e^{j\phi}$ is the complex channel gain, and the $\tilde{n}_{n,m}$ are the complex-valued Gaussian noise samples. For an ideal anti-aliasing filter having a cutoff frequency $1/(2T_s^g)$, the $\tilde{n}_{n,m}$ are independent zero-mean complex Gaussian random variables with variance $\sigma^2 = \frac{1}{2}\mathrm{E}[|\tilde{n}_{n,m}|^2] = N_o/T_s^g$, where $T_s^g = NT_s/(N+G)$.

Assuming a cyclic suffix as discussed in Sect. 4.6.1, the receiver first removes the guard interval according to

$$R_{n,m} = R_{n,G+(m-G)_N}^g,\ 0 \le m \le N-1, \tag{5.127}$$

where $(m)_N$ is the residue of m modulo N. Demodulation is then performed by computing the FFT on the block $\mathbf{R}_n = \{R_{n,m}\}_{m=0}^{N-1}$ to yield the vector $\mathbf{z}_n = \{z_{n,k}\}_{k=0}^{N-1}$ of N decision variables

$$\begin{aligned} z_{n,k} &= \frac{1}{N}\sum_{m=0}^{N-1} R_{n,m} e^{-\frac{j2\pi km}{N}} \\ &= gAx_{n,k} + v_{n,k}\ ,\ \ k = 0,\ldots,N-1, \end{aligned} \tag{5.128}$$

where $A = \sqrt{2E_h/T}$, $T = (N+G)T_s^g$, and the noise terms are given by

$$v_{n,k} = \frac{1}{N}\sum_{m=0}^{N-1} \tilde{n}_{n,m} e^{-\frac{j2\pi km}{N}}\ ,\ \ k = 0,\ldots,N-1. \tag{5.129}$$

It can be shown that the $v_{n,k}$ are zero-mean complex Gaussian random variables with covariance

$$\phi_{j,k} = \frac{1}{2}\mathrm{E}[v_{n,j}v_{n,k}^*] = \frac{N_o}{NT_s^g}\delta_{jk}. \tag{5.130}$$

Hence, the $z_{n,k}$ are independent Gaussian random variables with mean $g\sqrt{2E_h/T}x_{n,k}$ and variance N_o/NT_s^g. To be consistent with our earlier results for PSK and QAM signals, the $z_{n,k}$ can be multiplied for convenience by the scalar $\sqrt{NT_s^g}$. Such scaling gives

$$\tilde{z}_{n,k} = g\sqrt{2E_hN/(N+G)}x_{n,k} + \tilde{v}_{n,k}, \tag{5.131}$$

where the $\tilde{v}_{n,k}$ are i.i.d. zero-mean Gaussian random variables with variance N_o. Notice that $\sqrt{2E_hN/(N+G)}x_{n,k} = \tilde{s}_{n,k}$ is equal to the complex signal vector that is transmitted on the ith sub-carrier, where the term $N/(N+G)$ represents the loss in effective symbol energy due to the insertion of the cyclic guard interval. For *each* of the $\tilde{z}_{n,k}$, the receiver decides in favor of the *signal vector* $\tilde{s}_{n,k}$ that minimizes the squared Euclidean distance

$$\mu(\tilde{s}_{n,k}) = \|\tilde{z}_{n,k} - g\tilde{s}_{n,k}\|^2 \ , \quad k = 0, \ldots, N-1. \tag{5.132}$$

Thus, for each OFDM block, N symbol decisions must be made, one for each of the N sub-carriers. This can be done in either a serial fashion as in Fig. 5.14, or a parallel fashion. It is apparent from (5.131) that the probability of symbol error is identical to that achieved with independent modulation on each of the sub-carriers. This is expected, because the sub-carriers are mutually orthogonal in time.

5.7.1 Interchannel Interference

The above analysis assumes that the complex channel gain g remains constant over the OFDM symbol duration $T = NT_s = (N+G)T_s^g$. However, as the block size N increases and/or the maximum Doppler frequency increases for a fixed data rate $R_s = 1/T_s$, this assumption becomes invalid. The effect channel time variations on the OFDM link performance are now investigated. Although our analysis will be undertaken for flat fading channels, a similar analysis will apply to frequency selective channels provided that $G \geq L$. It will be shown that variations in the complex channel gain $\{g_k\}_{k=0}^{N-1}$ over the duration of an OFDM symbol cause interchannel interference (ICI) due to a loss of sub-channel orthogonality. The ICI will be shown to behave like additional AWGN that results in an error floor at high signal-to-noise ratios.

To isolate the Doppler effects, AWGN is ignored. The received discrete-time sequence after removal of the guard interval is

$$R_{n,m} = g_{G+(m-G)_N} X_{n,m}. \tag{5.133}$$

The vector $\mathbf{z}_n = \{z_{n,i}\}_{i=0}^{N-1}$ at the output of the FFT baseband demodulator is

$$z_{n,i} = \sqrt{2E_h/T} \sum_{m=0}^{N-1} x_{n,m} H(m-i), \tag{5.134}$$

where

$$H(m-i) = \frac{1}{N} \sum_{k=0}^{N-1} g_{G+(k-G)_N} \mathrm{e}^{\frac{j2\pi}{N}(m-i)k} \ , \quad 0 \leq i \leq N-1. \tag{5.135}$$

To highlight the effect of channel time variations, (5.134) can be rewritten as

$$z_{n,i} = \sqrt{2E_h/T} H(0) x_{n,i} + c_{n,i}, \tag{5.136}$$

where

$$c_{n,i} = \sqrt{2E_h/T} \sum_{\substack{m=0 \\ m \neq i}}^{N-1} x_{n,m} H(m-i). \tag{5.137}$$

Note that $H(0)$ is the *effective* complex channel gain, while $c_{n,i}$ is an additive noise term due to the ICI. Note that if the channel is time-invariant, then $g_k = g$ and $z_{n,i} = g\sqrt{2E_h/T}x_{n,i}$ as before.

If N is sufficiently large in (5.137), the central limit theorem can be invoked and the $c_{n,i}, i = 0, \ldots, N-1$ can be treated as complex Gaussian random variables that are characterized by their means, variances, and correlations. Since the $x_{n,m}$ and $H(m-i)$ are independent random variables and $\mathrm{E}[x_{n,m}] = 0$, it follows that $\mathrm{E}[c_l] = 0$. Since $2E_h \cdot \frac{1}{2}\mathrm{E}[x_{n,k}x_{n,m}^*] = E_{\mathrm{av}}\delta_{km}$, where E_{av} is the average symbol energy, the autocorrelation of the $c_{n,i}$ is

$$\phi_{cc}(r) = \frac{1}{2}\mathrm{E}[c_{n,i}c^*_{n,i+r}] = \frac{E_{\mathrm{av}}}{T}\sum_{m\neq i,i+r}\mathrm{E}[H(m-i)H^*(m-i-r)]. \tag{5.138}$$

Proceeding further requires a model for the time correlation of the channel. If the normalization $\mathrm{E}[|g_k|^2] = 1$ is assumed and Clarke's 2-D isotropic scattering model is assumed with an isotropic receiver antenna (see Chap. 2), then the autocorrelation becomes

$$\phi_{cc}(r) = \frac{E_{\mathrm{av}}}{T}\delta_r - \frac{E_{\mathrm{av}}}{TN^2}\sum_{k=0}^{N-1}\sum_{k'=0}^{N-1} J_0(2\pi f_m T_s^g(k-k'))\left(\mathrm{e}^{j\frac{2\pi k' r}{N}} + (1-\delta_r)\mathrm{e}^{j\frac{2\pi kr}{N}}\right), \tag{5.139}$$

where f_m is the maximum Doppler frequency.

For symbol-by-symbol detection, it is sufficient to examine the variance of the ICI term

$$\phi_{cc}(0) = \frac{E_{\mathrm{av}}}{T} - \frac{E_{\mathrm{av}}}{TN^2}\left(N + 2\sum_{i=1}^{N-1}(N-i)J_0(2\pi f_m T_s^g i)\right), \tag{5.140}$$

where the fact that $J_0(\,\cdot\,)$ is an even function has been used. Note that variance of the $c_{n,i}$ are only a function of E_{av}, N, T_s, and f_m, but is otherwise independent of the signal constellation. Figure 5.15 plots the signal-to-interference ratio, defined as

$$\mathrm{SIR} \triangleq \frac{E_{\mathrm{av}}/T}{\phi_{cc}(0)}, \tag{5.141}$$

as a function of $f_m T_s^g$ for several values of N. Observe that the SIR decreases as both the normalized Doppler maximum frequency $f_m T_s^g$ and the block size N increase.

Suppose that the data symbols $x_{n,k}$ are chosen from a 16-QAM alphabet. From Sect. 5.5, the symbol error probability for 16-QAM is

$$P_M = 3Q\left(\sqrt{\frac{1}{5}\gamma_s}\right)\left(1 - \frac{3}{4}Q\left(\sqrt{\frac{1}{5}\gamma_s}\right)\right), \tag{5.142}$$

where γ_s is the average received symbol energy-to-noise ratio. With Rayleigh fading, the symbol error probability is obtained by averaging (5.142) over the pdf in (5.86). Assuming validity of the Gaussian approximation for the ICI, the error floor due to ICI can be obtained by substituting the SIR in (5.141) for $\bar{\gamma}_s$. The results are shown in Fig. 5.16. Simulation results are also

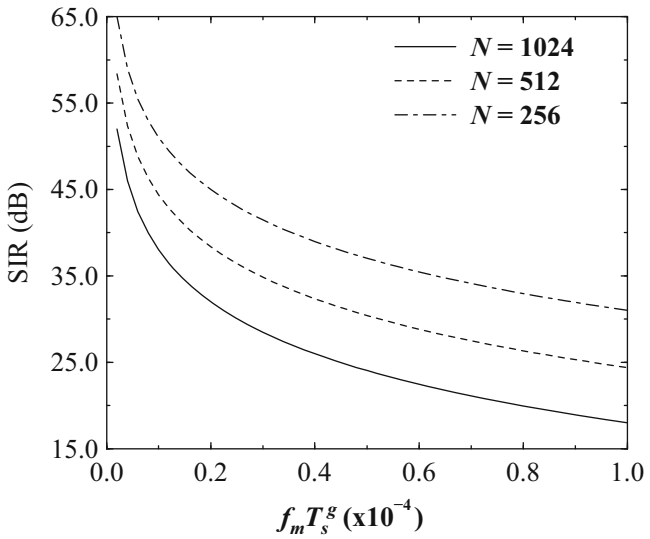

Fig. 5.15 Signal-to-interference ratio of OFDM due to ICI

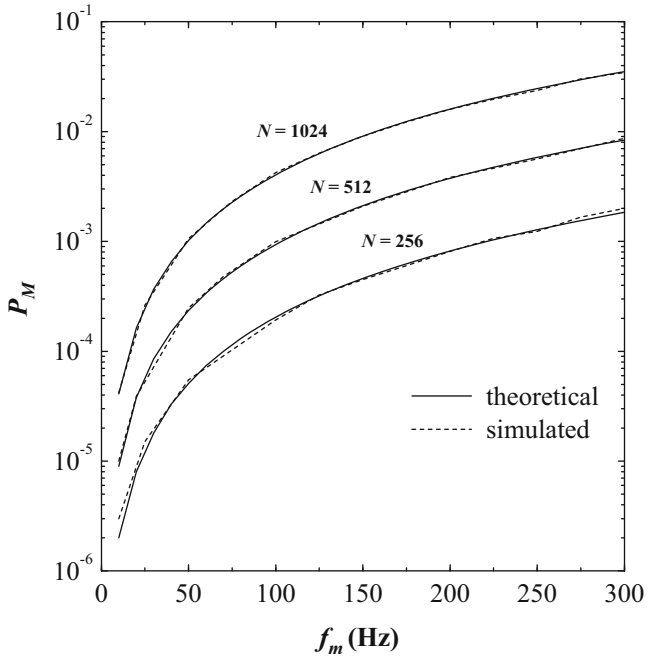

Fig. 5.16 Error floor due to ICI with 16-QAM

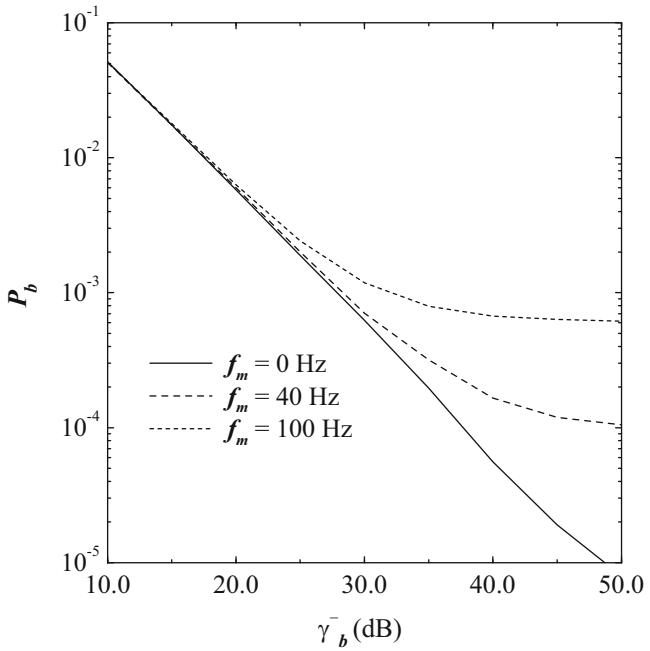

Fig. 5.17 Bit error probability for 16-QAM OFDM on a Rayleigh fading channel with various Doppler frequencies

shown in Fig. 5.16 corroborating the Gaussian approximation for the ICI. Figure 5.17 shows the bit error rate performance of OFDM with $N = 512$ sub-carriers, a 16-QAM signal constellation, and a 20 Mbps bit rate for various Doppler frequencies. At low $\bar{\gamma}_b$, additive noise dominates the performance so that the extra noise due to ICI has little effect. However, at large $\bar{\gamma}_b$ ICI dominates the performance and causes an error floor.

5.8 Differential Detection

Differentially encoded PSK (DPSK) can also be detected by using differentially coherent detection, where the receiver estimates the change in the excess phase of the received carrier between two successive baud intervals. Since DPSK transmits data in the differential excess carrier phase from one baud interval to the next, the basic mechanism for differential detection is obvious. For slow fading channels, the phase difference between waveforms received in two successive baud intervals will be independent of the absolute carrier phase. However for fast fading channels, the excess carrier phase will change over two successive baud intervals due to the channel. This leads to an error floor that increases with the fading rate.

5.8.1 Binary DPSK

Consider binary DPSK. Let θ_n denote the absolute transmitted excess carrier phase during the baud interval $nT \le t \le (n+1)T$, and let $\Delta\theta_n = \theta_n - \theta_{n-1}$ denote the differential excess carrier phase, where

$$\Delta\theta_n = \begin{cases} 0\ , & x_n = +1 \\ \pi\ , & x_n = -1 \end{cases}. \tag{5.143}$$

The DPSK complex envelope is

$$\tilde{s}(t) = A\sum_n h_a(t-nT)e^{j\theta_n} \tag{5.144}$$

and the received complex envelope is

$$\tilde{r}(t) = \alpha e^{j\phi} A\sum_n h_a(t-nT)e^{j\theta_n} + \tilde{n}(t), \tag{5.145}$$

where $g = \alpha e^{j\phi}$ is the complex channel gain. It is assumed that g changes slowly enough to remain essentially constant over two successive baud intervals.

A block diagram of a differentially coherent baseband demodulator for binary DPSK is shown in Fig. 5.18. During the time interval $nT \le t \le (n+1)T$, the values of X_n, X_{nd}, Y_n, and Y_{nd} in Fig. 5.18 are

$$\begin{aligned} X_n &= 2\alpha E_h \cos(\theta_n + \phi) + \tilde{n}_I \\ X_{nd} &= 2\alpha E_h \cos(\theta_{n-1} + \phi) + \tilde{n}_{I,d} \\ Y_n &= 2\alpha E_h \sin(\theta_n + \phi) + \tilde{n}_Q \\ Y_{nd} &= 2\alpha E_h \sin(\theta_{n-1} + \phi) + \tilde{n}_{Q,d}, \end{aligned} \tag{5.146}$$

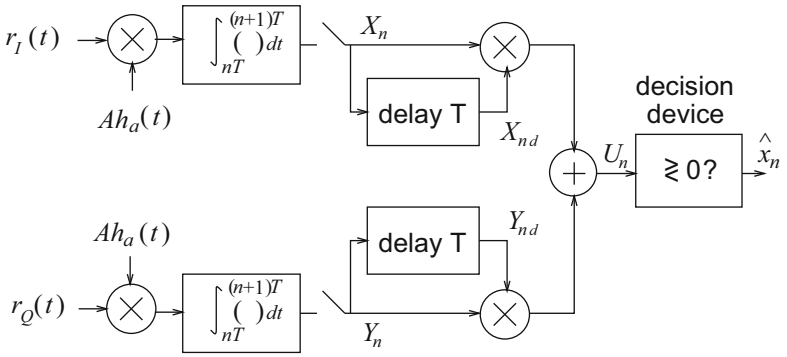

Fig. 5.18 Differentially coherent receiver for binary DPSK

where

$$E_h = \frac{A^2}{2}\int_0^T h_a^2(t)\mathrm{d}t \tag{5.147}$$

and the noise terms are

$$\begin{aligned}
\tilde{n}_I &= A\int_{nT}^{(n+1)T} \tilde{n}_I(t)h_a(t)\mathrm{d}t \\
\tilde{n}_{I,d} &= A\int_{(n-1)T}^{nT} \tilde{n}_I(t)h_a(t)\mathrm{d}t \\
\tilde{n}_Q &= A\int_{nT}^{(n+1)T} \tilde{n}_Q(t)h_a(t)\mathrm{d}t \\
\tilde{n}_{Q,d} &= A\int_{(n-1)T}^{nT} \tilde{n}_Q(t)h_a(t)\mathrm{d}t.
\end{aligned} \tag{5.148}$$

One can show that $\tilde{n}_I$, $\tilde{n}_{I,d}$, $\tilde{n}_Q$, and $\tilde{n}_{Q,d}$ are independent identically distributed zero-mean Gaussian random variables with variance $2E_hN_o$.

In the absence of noise, it is easy to verify that the input to the decision device is $U_n = 4\alpha^2E_h^2x_n$. Hence, the sign of U_n is equal to the sign of x_n and correct decisions are made. When noise is present, U_n is a random variable, and to determine the probability of error the pdf of U_n is required. To determine the pdf of the U_n, it is convenient to express U_n as

$$U_n = \mathrm{Re}\left\{Z_nZ_{nd}^*\right\} = \frac{1}{2}\left(Z_nZ_{nd}^* + Z_n^*Z_{nd}\right) \tag{5.149}$$

where

$$Z_n = X_n + jY_n \tag{5.150}$$

$$Z_{nd} = X_{nd} + jY_{nd}. \tag{5.151}$$

It can be shown by using characteristic functions that U_n has the differential form $U_n = W_n - Y_n$, where W_n and Y_n are non-central and central chi-square random variables with respective densities [308]

$$f_{W_n}(w) = \frac{1}{2E_hN_o}\exp\left\{-\frac{(wx_n + 4\alpha^2E_h^2)}{2E_hN_o}\right\} I_0\left(\frac{2\sqrt{wx_n\alpha^2E_h^2}}{E_hN_o}\right), \quad wx_n \geq 0 \tag{5.152}$$

$$f_{Y_n}(y) = \frac{1}{2E_hN_o}\exp\left\{-\frac{yx_n}{2E_hN_o}\right\}, \quad yx_n \geq 0, \tag{5.153}$$

where $I_0(x)$ is the zero-order modified Bessel function of the first kind defined by

$$I_0(x) = \frac{1}{2\pi}\int_0^{2\pi} \mathrm{e}^{-x\cos\theta}\mathrm{d}\theta. \tag{5.154}$$

By defining the auxiliary random variable $V_n = W_n$ and using a bivariate transformation of random variables, the pdf of U_n is

$$\begin{aligned}
f_{U_n}(u) &= \int_{R_{U_nV_n}} f_{W_n}(v)f_{Y_n}(v-u)\mathrm{d}v \\
&= \begin{cases}
\frac{1}{4E_hN_o}\exp\left\{\frac{x_nu-2\alpha^2E_h^2}{2E_hN_o}\right\} & , -\infty < x_nu < 0 \\
\frac{1}{4E_hN_o}\exp\left\{\frac{x_nu-2\alpha^2E_h^2}{2E_hN_o}\right\} Q\left(\sqrt{\frac{2\alpha^2E_h}{N_o}}, \sqrt{\frac{2x_nu}{E_hN_o}}\right) & , 0 < x_nu < \infty
\end{cases},
\end{aligned} \tag{5.155}$$

where $Q(a, b)$ is the Marcum Q function, defined by

$$Q(a,b) = 1 - \int_0^b z\mathrm{e}^{-\frac{z^2+a^2}{2}} I_0(za)\,\mathrm{d}z. \tag{5.156}$$

From (5.155), the bit error probability of DPSK with differential detection is

$$P_b(\gamma_b) = \int_0^\infty \frac{1}{4E_hN_o}\exp\left\{-\frac{u+2\alpha^2E_h^2}{2E_hN_o}\right\}\mathrm{d}u = \frac{1}{2}\mathrm{e}^{-\gamma_b}, \tag{5.157}$$

where $\gamma_b = \alpha^2E_h/N_o$ is the received bit energy-to-noise ratio. For a slow Rayleigh fading channel, α is Rayleigh distributed so the received bit energy-to-noise ratio, γ_b, has the exponential pdf in (5.85). It follows that the average bit error probability with slow Rayleigh fading is

$$P_b = \int_0^\infty P_b(x)p_{\gamma_b}(x)dx = \frac{1}{2(1+\bar{\gamma}_b)} \approx \frac{1}{2\bar{\gamma}_b}. \tag{5.158}$$

Note that the error probability has an inverse linear dependency on $\bar{\gamma}_b$.

5.8.2 *Differential Detection of π/4-DQPSK*

Differential detection can be used with $\pi/4$-DQPSK as well. Once again the complex envelopes of the transmitted and received signals are given by (5.144) and (5.145), respectively. However, with $\pi/4$-DQPSK, $\Delta\theta_n = \pi x_n/4$ where $x_n \in \{\pm1, \pm3\}$, so that one of the four possible differential phases must be detected. A block diagram of a differentially coherent baseband demodulator for $\pi/4$-DQPSK is shown in Fig. 5.19. The values of X_n, X_{nd}, Y_n, and Y_{nd} are again given by (5.146). The detector outputs are

$$U_n = \mathrm{Re}\left\{Z_nZ_{nd}^*\right\} = \frac{1}{2}\left(Z_nZ_{nd}^* + Z_n^*Z_{nd}\right) \tag{5.159}$$

$$V_n = \mathrm{Im}\left\{Z_nZ_{nd}^*\right\} = \frac{1}{j2}\left(Z_nZ_{nd}^* - Z_n^*Z_{nd}\right), \tag{5.160}$$

where Z_n and Z_{nd} are defined in (5.150) and (5.151), respectively. In the absence of noise, it can be verified that the detector outputs are

$$\begin{aligned} U_n &= -a, \quad V_n = -a, \quad \text{for } x_n = -3 \\ U_n &= a, \quad V_n = -a, \quad \text{for } x_n = -1 \\ U_n &= a, \quad V_n = a, \quad \text{for } x_n = +1 \\ U_n &= -a, \quad V_n = a, \quad \text{for } x_n = +3 \end{aligned} \tag{5.161}$$

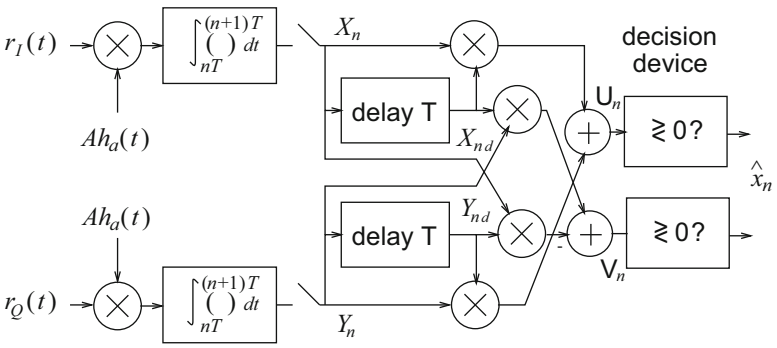

Fig. 5.19 Differentially coherent receiver for $\pi/4$-DQPSK

where $a = 2\sqrt{2}\alpha^2 E_h^2$. The bit error probability for $\pi/4$-DQPSK with Gray coding is somewhat complicated to derive and omitted here, but can be expressed in terms of well-known functions [272]

$$P_b(\gamma_b) = Q(a, b) - \frac{1}{2} I_0(ab) \mathrm{e}^{-\frac{1}{2}(a^2+b^2)}, \tag{5.162}$$

where

$$a = \sqrt{2\gamma_b \left(1 - \frac{1}{\sqrt{2}}\right)} \tag{5.163}$$

$$b = \sqrt{2\gamma_b \left(1 + \frac{1}{\sqrt{2}}\right)} \tag{5.164}$$

and γ_b is the bit energy-to-noise ratio. Once again, if the channel is flat faded, then the bit error probability can be obtained by averaging (numerically) over the distribution of γ_b in (5.85).

5.9 Non-coherent Detection

If information is transmitted in the amplitude and/or frequency of a waveform, but not the phase, then a non-coherent receiver can be used. Non-coherent receivers make no attempt to determine the carrier phase and are, therefore, easier to implement than coherent receivers. Non-coherent receivers generally trade implementation complexity and robustness to channel impairments, such as high Doppler conditions, for transmitter power and/or bandwidth.

Suppose that one of the M complex low-pass waveforms, $\tilde{s}_m(t), m = 1, \ldots, M$, say $\tilde{s}_i(t)$, is transmitted on a flat fading channel with AWGN. The received complex envelope is

$$\tilde{r}(t) = g\tilde{s}_i(t) + \tilde{n}(t), \tag{5.165}$$

where $g = \alpha e^{j\phi}$ is the channel gain that includes the random phase ϕ, and $\tilde{n}(t)$ is the AWGN. By projecting $\tilde{r}(t)$ onto the set of basis functions $\{\varphi_n(t)\}_{n=1}^N$ obtained through the Gram–Schimdt orthonormalization procedure, the received vector is obtained as

$$\tilde{\mathbf{r}} = g\tilde{\mathbf{s}}_i + \tilde{\mathbf{n}}, \tag{5.166}$$

where the joint pdf of $\tilde{\mathbf{n}}$ is given in (5.13).

The maximum likelihood (ML) non-coherent detector does not require knowledge of the random excess received carrier phase ϕ in the decision process, and chooses the message vector $\tilde{\mathbf{s}}_m$ that maximizes the joint conditional pdf $p(\tilde{\mathbf{r}}|\alpha, \tilde{\mathbf{s}}_m)$:

$$\text{choose } \tilde{\mathbf{s}}_m \text{ if } \quad p(\tilde{\mathbf{r}}|\alpha, \tilde{\mathbf{s}}_m) \geq p(\tilde{\mathbf{r}}|\alpha, \tilde{\mathbf{s}}_{\hat{m}}) \ \ \forall \hat{m} \neq m. \tag{5.167}$$

Letting $p(\phi)$ denote the pdf of ϕ,

$$p(\tilde{\mathbf{r}}|\alpha, \tilde{\mathbf{s}}_m) = \mathrm{E}_\phi[p(\tilde{\mathbf{r}}|g, \tilde{\mathbf{s}}_m)] = \int_0^{2\pi} p(\tilde{\mathbf{r}}|g, \tilde{\mathbf{s}}_m) p(\phi) d\phi. \tag{5.168}$$

Using the joint conditional pdf of $p(\tilde{\mathbf{r}}|g, \tilde{\mathbf{s}}_m)$ in (5.20) yields

$$\begin{aligned} p(\tilde{\mathbf{r}}|g, \tilde{\mathbf{s}}_m) &= \frac{1}{(2\pi N_o)^N} \exp\left\{-\frac{1}{2N_o} \|\tilde{\mathbf{r}} - g\tilde{\mathbf{s}}_m\|^2\right\} \\ &= \frac{1}{(2\pi N_o)^N} \exp\left\{-\frac{\|\tilde{\mathbf{r}}\|^2 + 2\alpha^2 E_m}{2N_o}\right\} \exp\left\{\frac{1}{N_o} \mathrm{Re}\{\tilde{\mathbf{r}} \cdot g^* \tilde{\mathbf{s}}_m^*\}\right\}, \end{aligned} \tag{5.169}$$

where, again, E_m is the energy in the bandpass waveform $s_m(t)$ corresponding to the signal vector $\tilde{\mathbf{s}}_m$. Next let $\tilde{\mathbf{r}} \cdot \tilde{\mathbf{s}}_m^* = X_m e^{j\theta_m}$ so that

$$\tilde{\mathbf{r}} \cdot g^* \tilde{\mathbf{s}}_m^* = g^* \tilde{\mathbf{r}} \cdot \tilde{\mathbf{s}}_m^* = g^* X_m^{j\theta_m} = \alpha X_m e^{j(\theta_m - \phi)}. \tag{5.170}$$

Hence,

$$p(\tilde{\mathbf{r}}|g, \tilde{\mathbf{s}}_m) = \frac{1}{(2\pi N_o)^N} \exp\left\{-\frac{\|\tilde{\mathbf{r}} + 2\alpha^2 E_m\|^2}{2N_o}\right\} \exp\left\{\frac{\alpha X_m}{N_o} \cos(\theta_m - \phi)\right\}. \tag{5.171}$$

In the absence of any prior information, the random phase ϕ is assumed to be uniformly distributed on $[-\pi, \pi)$, resulting in

$$\begin{aligned} p(\tilde{\mathbf{r}}|\alpha, \tilde{\mathbf{s}}_m) &= \frac{1}{(2\pi N_o)^N} \exp\left\{-\frac{2\alpha^2 E_m + \|\tilde{\mathbf{r}}\|^2}{2N_o}\right\} \frac{1}{2\pi} \int_0^{2\pi} \exp\left\{\frac{\alpha X_m}{N_o} \cos(\theta_m - \phi)\right\} \mathrm{d}\phi \\ &= \frac{1}{(2\pi N_o)^N} \exp\left\{-\frac{2\alpha^2 E_m + \|\tilde{\mathbf{r}}\|^2}{2N_o}\right\} I_0\left(\frac{\alpha X_m}{N_o}\right). \end{aligned} \tag{5.172}$$

Since the terms $\|\tilde{\mathbf{r}}\|^2$ and $(2\pi N_o)^N$ are independent of the choice of $\tilde{\mathbf{s}}_m$, the signal vector that maximizes $p(\tilde{\mathbf{r}}|\alpha, \tilde{\mathbf{s}}_m)$ also maximizes the decision metric

$$\mu_1(\mathbf{s}_m) = \exp\left\{-\frac{\alpha^2 E_m}{N_o}\right\} I_0\left(\frac{\alpha X_m}{N_o}\right). \tag{5.173}$$

If all message waveforms have equal energy, then considerable simplification will result. In this case, the ML receiver can choose $\tilde{\mathbf{s}}_m$ to maximize

$$\mu_2(\tilde{\mathbf{s}}_m) = I_0\left(\frac{\alpha X_m}{N_o}\right). \tag{5.174}$$

However, $I_0(x)$ increases monotonically with x. Therefore, the ML receiver can simply choose $\tilde{\mathbf{s}}_m$ to maximize

$$\mu_3(\tilde{\mathbf{s}}_m) = X_m. \tag{5.175}$$

From the above development, the structure of the ML non-coherent receiver is clear. The receiver first uses the quadrature demodulator in Fig. 5.1 to extract the real and imaginary components of the complex envelope $\tilde{r}_I(t)$ and $\tilde{r}_Q(t)$. Then it computes the received signal vector $\mathbf{r}$ using the correlator detector in Fig. 5.2 or matched filter detector in Fig. 5.3. For equal energy messages, the decision variables $X_m = |\tilde{\mathbf{r}} \cdot \tilde{\mathbf{s}}_m^*|$, $m = 1, \ldots, M$, are computed and the signal vector $\tilde{\mathbf{s}}_m$ is chosen that has the largest X_m. If the messages do not have equal energy, then the metric in (5.173) must be used instead. This will add considerable complexity to the ML receiver, because the channel gain α must be determined and the Bessel function $I_0(x)$ must be calculated. Finally,

$$X_m = \left[\mathrm{Re}^2(\tilde{\mathbf{r}} \cdot \tilde{\mathbf{s}}_m^*) + \mathrm{Im}^2(\tilde{\mathbf{r}} \cdot \tilde{\mathbf{s}}_m^*)\right]^{1/2}. \tag{5.176}$$

This leads to the detector structure shown in Fig. 5.20, commonly known as a square-law detector. Note that the square-law detector generates X_m^2, $m = 1, \ldots, M$ rather than X_m, $m = 1, \ldots, M$. However, the choice of $\tilde{\mathbf{s}}_m$ that maximizes X_m^2 also maximizes X_m.

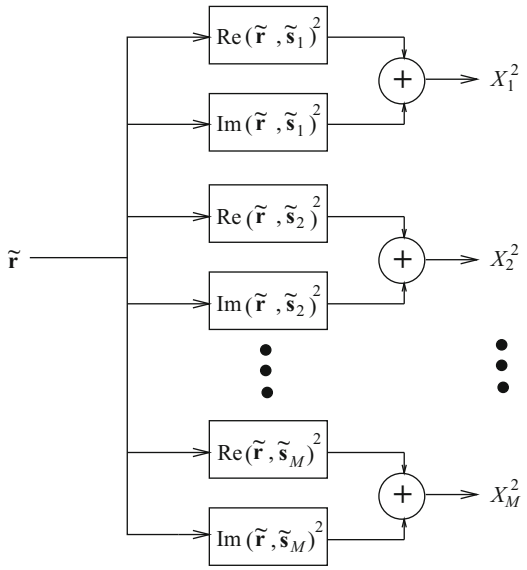

Fig. 5.20 Non-coherent square-law detector

5.9.1 *Error Probability of M-ary Orthogonal Signals*

Consider the case of M-ary orthogonal signals as discussed in Sect. 4.5. Assume without loss of generality that $\tilde{\mathbf{s}}_1$ is sent. Then the received vector $\tilde{\mathbf{r}} = (\tilde{r}_1, \tilde{r}_2, \ldots, \tilde{r}_N)$ has components

$$\begin{aligned} \tilde{r}_1 &= g\sqrt{2E} + \tilde{n}_1 \\ \tilde{r}_i &= \tilde{n}_i\,, \quad i = 2, \ldots, M. \end{aligned} \tag{5.177}$$

Since the M-ary orthogonal signals have equal energy, the metric in (5.175) can be used. Then

$$\begin{aligned} X_1 &= |\tilde{\mathbf{r}} \cdot \tilde{\mathbf{s}}_1^*| \\ &= |2Eg + \sqrt{2E}\tilde{n}_1| \\ &= \left|2E\alpha\cos(\phi) + \sqrt{2E}\tilde{n}_{I,1} + j\left(2E\alpha\sin(\phi) + \sqrt{2E}\tilde{n}_{Q,1}\right)\right| \end{aligned} \tag{5.178}$$

and

$$\begin{aligned} X_m &= |\tilde{\mathbf{r}} \cdot \tilde{\mathbf{s}}_m^*| \\ &= |\sqrt{2E}\tilde{n}_m| \\ &= \left|\sqrt{2E}\tilde{n}_{I,m} + j\sqrt{2E}\tilde{n}_{Q,m}\right|\,, \quad m = 2, \ldots, M. \end{aligned} \tag{5.179}$$

The receiver will make a correct decision if

$$X_1 > X_i\,, \quad \forall\, i \neq 1. \tag{5.180}$$

From Appendix A, X_1 has the Rice distribution

$$p_{X_1}(x) = \frac{x}{2EN_o}\exp\left\{-\frac{x^2 + 4\alpha^2E^2}{4EN_o}\right\} I_0\left(\frac{\alpha x}{N_o}\right), \tag{5.181}$$

while the $X_i, i \neq 0$, are independent Rayleigh random variables with pdf

$$p_{X_i}(x) = \frac{x}{2EN_o}\exp\left\{-\frac{x^2}{4EN_o}\right\} \quad , \quad i = 2, \ldots, M. \tag{5.182}$$

The probability of correct symbol reception is

$$\begin{aligned} \mathrm{P}[c] &= \mathrm{P}\left[X_2 < X_1, X_3 < X_1, \ldots, X_M < X_1\right] \\ &= \int_0^\infty \left(\int_0^y \frac{x}{2EN_o}\exp\left\{-\frac{x^2}{4EN_o}\right\} \mathrm{d}x\right)^{M-1} p_{X_1}(y)\mathrm{d}y \\ &= \int_0^\infty \left(1 - \exp\left\{-\frac{y^2}{4EN_o}\right\}\right)^{M-1} p_{X_1}(y)\mathrm{d}y. \end{aligned} \tag{5.183}$$

Using the binomial expansion

$$(1-x)^n = \sum_{k=0}^{n} \binom{n}{k} (-1)^k x^k$$

gives

$$\mathrm{P}[c] = \sum_{k=0}^{M-1} (-1)^k \binom{M-1}{k} \int_0^\infty \exp\left\{-\frac{ky^2}{4EN_o}\right\} p_{X_1}(y)\mathrm{d}y. \tag{5.184}$$

The integral in the above expression is

$$\begin{aligned} \mathscr{I} &= \int_0^\infty \exp\left\{-\frac{ky^2}{4EN_o}\right\} p_{X_1}(y)\mathrm{d}y \\ &= \int_0^\infty \exp\left\{-\frac{ky^2}{4EN_o}\right\} \frac{y}{2EN_o}\exp\left\{-\frac{y^2 + 4\alpha^2E^2}{4EN_o}\right\} I_0\left(\frac{\alpha y}{N_o}\right)\mathrm{d}y \\ &= \int_0^\infty \frac{y}{2EN_o}\exp\left\{-\frac{(k+1)y^2 + 4\alpha^2E^2}{4EN_o}\right\} I_0\left(\frac{\alpha y}{N_o}\right)\mathrm{d}y. \end{aligned} \tag{5.185}$$

The trick is to manipulate the integrand of $\mathscr{I}$ into the product of a Ricean pdf and a term that does not depend on the variable of integration y. This is accomplished by making the substitutions

$$N_o' = \frac{2EN_o}{k+1} \qquad\qquad E' = \frac{E}{(k+1)} \tag{5.186}$$

and solving the integral. This gives

$$\mathscr{I} = \frac{1}{k+1}\exp\left\{-\frac{2k\alpha^2E'^2}{N_o'}\right\} = \frac{1}{k+1}\exp\left\{-\frac{k\gamma_s}{(k+1)}\right\}, \tag{5.187}$$

where $\gamma_s = \alpha^2E/N_o$ is the symbol energy-to-noise ratio. Hence, the probability of correct symbol reception is

$$\mathrm{P}[c] = \sum_{k=0}^{M-1} \frac{(-1)^k\binom{M-1}{k}}{k+1}\exp\left\{-\frac{k\gamma_s}{(k+1)}\right\} \tag{5.188}$$

and the probability of symbol error is

$$P_M = 1 - \mathrm{P}[c] = \sum_{k=1}^{M-1} \frac{(-1)^{k+1}\binom{M-1}{k}}{k+1} \exp\left\{-\frac{k\gamma_s}{(k+1)}\right\}. \tag{5.189}$$

For orthogonal signals $\gamma_s = \gamma_b \log_2 M$ and the bit error probability is given by (5.56). Hence,

$$P_b(\gamma_b) = \frac{M}{2(M-1)} \sum_{k=1}^{M-1} \frac{(-1)^{k+1}\binom{M-1}{k}}{k+1} \exp\left\{-\frac{k\gamma_b \log_2 M}{(k+1)}\right\}. \tag{5.190}$$

For Rayleigh fading channels, the error probability can be averaged over the distribution of γ_b in (5.85). This gives the following simple closed form for the average bit error probability

$$P_b = \frac{M}{2(M-1)} \sum_{k=1}^{M-1} \frac{(-1)^{k+1}\binom{M-1}{k}}{1+k+k\bar{\gamma}_b \log_2 M}. \tag{5.191}$$

Once again, the error probability has an inverse linear dependency on $\bar{\gamma}_b$.

5.10 Detection of CPM Signals

CPM receivers can be categorized into three different types of detection schemes: coherent detection, differential detection, and non-coherent detection. Furthermore, in each category there are two approaches: symbol-by-symbol detectors and sequence estimators. Sequence estimators will be treated in the context of channel coding in Chap. 8. This section only considers symbol-by-symbol CPM detectors. While there exist a large variety of coherent and non-coherent symbol-by-symbol CPM detectors, we present two structures. Both receiver structures use multiple-symbol observation intervals to detect partial response CPM signals, and both generate soft outputs making them well suited to systems that employ convolutional, trellis, or Turbo coding.

Recall that the partial response CPM complex envelope during the time interval $nT \le t \le (n+1)T$ is, from (4.133),

$$\tilde{s}(t) = A e^{j\left(\theta_n + 2\pi h \sum_{k=n-L+1}^{n} x_n \beta(t-kT)\right)}, \tag{5.192}$$

and the CPM state at time $t = nT$ is defined by the L-tuple

$$S_n = (\theta_n, x_{n-1}, x_{n-2}, \cdots, x_{n-L+1}). \tag{5.193}$$

In the sequel, the CPM complex envelope during the time interval $nT \le t \le (n+1)T$ will also be denoted by $\tilde{s}(S_n, x_n, t)$ to emphasize the finite state nature of the signal. For a slow flat fading channel, the received signal is

$$\tilde{r}(t) = g\tilde{s}(t) + \tilde{n}(t), \tag{5.194}$$

where $\tilde{n}(t)$ is a zero-mean complex AWGN with psd N_o watts/Hz.

5.10.1 Coherent Detection and Error Probability of MSK and GMSK

MSK signals can be recovered using a variety of detection techniques. One method uses the linear representation of MSK, where MSK is equivalent to OQASK with a half-sinusoid amplitude shaping function as described in (4.111)–(4.116). The received complex envelope is

$$\tilde{r}(t) = g\tilde{s}(t) + \tilde{n}(t), \tag{5.195}$$

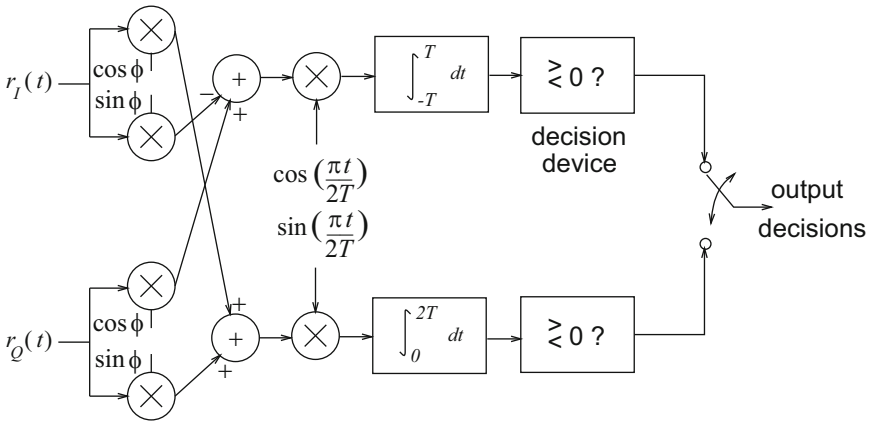

Fig. 5.21 Coherent detector for MSK signals

where $g = \alpha e^{j\phi}$. A coherent MSK receiver first removes the effect of the channel phase rotation according to

$$\begin{aligned} e^{-j\phi}\tilde{r}(t) &= \tilde{r}_I(t)\cos(\phi) + \tilde{r}_Q(t)\sin(\phi) + j\Big(\tilde{r}_Q(t)\cos(\phi) - \tilde{r}_I(t)\sin(\phi)\Big) \\ &= \alpha\tilde{s}_I(t) + \tilde{n}_I(t) + j\Big(\alpha\tilde{s}_Q(t) + \tilde{n}_Q(t)\Big), \end{aligned} \tag{5.196}$$

where the effect of the phase rotation on the noise $\tilde{n}(t)$ has been ignored due to its circular symmetry. Detection then proceeds by processing the real and imaginary parts of $e^{-j\phi}\tilde{r}(t)$ as orthogonal binary PAM streams. The resulting MSK detector is shown in Fig. 5.21. Note that the source symbols on the in-phase and quadrature carrier components must be detected over intervals of length $2T$, the duration of the half-sinusoid amplitude shaping pulse $h_a(t)$, and bit decisions are made every T seconds. It follows that coherently detected MSK has the same bit error rate performance as QPSK, OQPSK, and BPSK.

By using the linearized representation of GMSK, LGMSK, in Sect. 4.8.3, replaces the half-sinusoid amplitude shaping pulse in (4.8.3) with the LGMSK pulse in (4.157). This will create ISI that will degrade performance somewhat if a matched filter with symbol-by-symbol decisions are used. For example, with $BT = 0.25$, the E_b/N_o degradation is roughly 0.75 dB in AWGN [122]. The induced ISI can be mitigated by using a variety of channel equalization techniques for linear modulation schemes as detailed in Chap. 7, such that the performance loss due to the Gaussian pulse shaping is negligible.

5.10.2 Coherent CPM Demodulator

A coherent CPM demodulator was proposed by Osborn and Luntz [252], and Schonhoff [295]. The decision metrics for symbol x_n are obtained by observing $\tilde{r}(t)$ over $N_p + 1$ successive symbol intervals and generating decision metrics for all M^{N_p+1} possible symbol vectors $\mathbf{x}_n = \{x_n, \mathbf{b}_n\}$, where $\mathbf{b}_n = \{x_{n+1}, \cdots, x_{n+N_p}\}$. The ML metric for x_n is proportional to the conditional density $p(\tilde{r}(t)|S_n, x_n, \mathbf{b}_n, g)$ and is given by

$$\mu(S_n, x_n, \mathbf{b}_n) = -\sum_{i=n}^{n+N_p} \int_{iT}^{(i+1)T} |\tilde{r}(t) - g\tilde{s}(S_i, x_i, t)|^2 dt. \tag{5.197}$$

The metrics for x_n can be obtained by averaging (5.197) over the M^{N_p} possible values of $\mathbf{b}_n$ and averaging over all possible initial states S_n. This leads to the decision metric

$$\mu(x_n) = \sum_{S_n}\sum_{\mathbf{b}_n} \mu(S_n, x_n, \mathbf{b}_n)\mathrm{P}[\mathbf{b}_n]\mathrm{P}[S_n] = \sum_{S_n}\sum_{\mathbf{b}_n} \mu(S_n, x_n, \mathbf{b}_n)\ , \tag{5.198}$$

where $\mathrm{P}[\mathbf{b}_n]$ and $\mathrm{P}[S_n]$ are the probabilities of $\mathbf{b}_n$ and S_n, respectively, and the last equality follows because all the $\mathbf{b}_n$ are equally likely, and all the S_n are equally likely, for equally likely data symbols. By using (5.198) a set of M metrics is calculated for the M possible x_n. The receiver makes the final decision by choosing the symbol having the largest decision metric.

A simplified receiver that will yield almost the same performance uses the suboptimum decision metric [252, 295]

$$\mu(x_n) = \max_{S_n} \max_{\mathbf{b}_n} \left\{ -\sum_{i=n}^{n+N_p} \int_{iT}^{(i+1)T} |\tilde{r}(t) - g\tilde{s}(S_i, x_i, t)|^2 \mathrm{d}t \right\}, \tag{5.199}$$

which is also exactly the same as the decision metric proposed by Kerr and McLane for full response CPFSK [180]. Once again, by using (5.199) a set of M decision metrics is calculated for the M possible x_n and the receiver chooses the symbol having the largest decision metric.

5.10.3 Non-coherent CPM Demodulator

A non-coherent receiver can be constructed by using a multiple-symbol observation interval similar to that suggested for the coherent receiver described in the previous section [368]. After observing $\tilde{r}(t)$ over the N-symbol interval $(n - n_1)T \le t \le (n + n_2)T$, where $N = n_1 + n_2 + 1$, the non-coherent CPM demodulator in [368] generates the following set of M^{N+L-2} conditional symbol metrics for each x_n:

$$\mu(x_n, \mathbf{b}_n) = \left| \sum_{i=n-n_1}^{n+n_2} \int_{iT}^{(i+1)T} \tilde{r}(t)\tilde{s}^*(S_i, x_i, t)\, \mathrm{d}t \right|^2, \tag{5.200}$$

where $\mathbf{b}_n = \{x_{n-n_1-L+1}, \cdots, x_{n-1}, x_{n+1}, \cdots, x_{n+n_2}\}$ is the "adjacent" symbol vector that excludes x_n. Note that the phase term θ_{n-n_1} in S_{n-n_1} does not affect the value of (5.200) and can, therefore, be assumed zero. A simple symbol metric can be formed by choosing the largest among all possible $\mu(x_n, \mathbf{b}_n)$, viz.,

$$\mu(x_n) = \max_{\mathbf{b}_n} \left| \sum_{i=n-n_1}^{n+n_2} \int_{iT}^{(i+1)T} \tilde{r}(t)\tilde{s}^*(S_i, x_i, t)\, \mathrm{d}t \right|^2. \tag{5.201}$$

The set of M symbol metrics so obtained is then used to make decisions on the transmitted symbols by selecting the symbol with the largest symbol metric.

For $N = 1$ ($n_1 = n_2 = 0$), the symbol metric in (5.201) is the same one used by the single-symbol receiver in [5] and, as a result, the single-symbol receiver can be treated as a special case of the receiver presented here. In order to calculate the metrics in an efficient recursive fashion, an approach similar to [304] can be followed to rewrite $\mu(x_n, \mathbf{b}_n)$ as

$$\mu(x_n, \mathbf{b}_n) = \left| \sum_{i=n-n_1}^{n+n_2} \Gamma_i F_i \right|^2, \tag{5.202}$$

where

$$\begin{aligned} \Gamma_i &= \int_{iT}^{(i+1)T} \tilde{r}(t)\tilde{s}^*(x_{i-L+1}, \cdots, x_i, t)\, \mathrm{d}t \\ F_i &= \mathrm{e}^{-j\pi h x_{i-L}} F_{i-1}; \quad F_{n-n_1} = 1. \end{aligned} \tag{5.203}$$

The metric generator structure is shown in Fig. 5.22. Generally, the metric calculator requires M^L matched filters and generates M^{N+L-1} conditional symbol metrics $\mu(x_n, \mathbf{b}_n)$. However, unlike the coherent receiver, the complexity is independent of the modulation index h. Actually, since the term θ_n is not explicitly exploited in S_n, h is not even required to be a rational number, i.e., the CPM waveform is not required to have a finite number of states. Finally, it is observed that the complex channel gain g is not required and, therefore, the receiver complexity is greatly reduced.

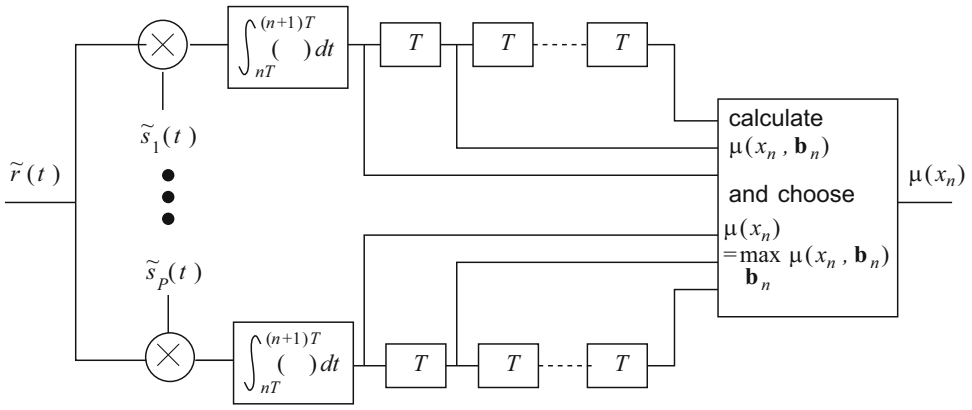

Fig. 5.22 The symbol metric calculator. Note that the signal $\tilde{s}^*(t)$ is labeled to account for $P = M^L$ possible matched filters

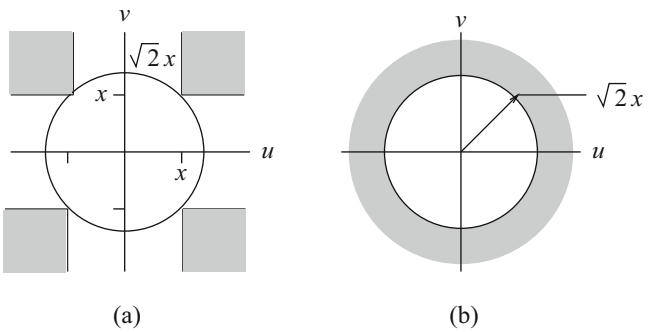

Fig. 5.23 Figure for Problem 5.1

Problems

5.1. Derive the upper bound

$$Q(x) \leq \frac{1}{2}\mathrm{e}^{-x^2/2}, \qquad x \geq 0.$$

Hint: Note that $4Q^2(x)$ is the probability that a pair of independent zero mean, unit variance, Gaussian random variables u, v lie within the shaded region of Fig. 5.23a. This probability is exceeded by the probability that u, v lies within the shaded region of Fig. 5.23b.

5.2. Consider the receiver model shown in Fig. 5.24, consisting of a linear time-invariant filter $h_r(t)$ followed by a sampler. The input to the filter consists of a pulse $h_a(t)$ of duration T corrupted by AWGN

$$\tilde{r}(t) = h_a(t) + \tilde{n}(t), \quad 0 \leq t \leq T.$$

The output of the filter is

$$\tilde{y}(t) = p(t) + \tilde{z}(t)$$

where $p(t) = h_a(t) * h_r(t)$ and $\tilde{z}(t) = \tilde{n}(t) * h_r(t)$, the filter output is sampled at time T to produce the sample $y(T) = p(T) + \tilde{z}(T)$. The signal-to-noise ratio at the output of the sampler is defined as

$$\mathrm{SNR} = \frac{|p(T)|^2}{\mathrm{E}[|\tilde{z}(T)|^2]}.$$

Find the filter $h_r(t)$, and corresponding transfer function $H_r(f)$, that will maximize the SNR.

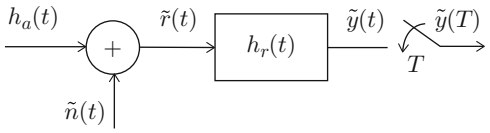

Fig. 5.24 Figure for Problem 5.2

5.3. Consider the pulse

$$h_a(t) = \begin{cases} \sin\left(\frac{4\pi t}{T}\right), & 0 \le t \le T \\ 0, & \text{otherwise} \end{cases}.$$

(a) Determine the impulse response of the matched filter for this signal.
(b) Sketch the waveform $y(t)$ at the output of the matched filter, and determine the output value at time $t = T$.
(c) Sketch the waveform $y(t)$ at the output of a correlator that correlates $h_a(t)$ with itself, and determine the output value at time $t = T$.

5.4. Derive the expression for the symbol error probability of $\sqrt{M}$-PAM in (5.102).

5.5. Show that the symbol error probability for coherent M-ary PSK is bounded by $p \le P_M \le 2p$, where

$$p = Q\left(\sqrt{2\gamma_s}\sin\frac{\pi}{M}\right)$$

and γ_s is the symbol energy-to-noise ratio.

5.6. Suppose that BPSK signaling is used with coherent detection. The channel is affected by flat Rayleigh fading and log-normal shadowing with a shadow standard deviation of σ_Ω dB. The composite squared-envelope has the probability density in (2.371).

(a) Obtain an expression for the probability density function of the composite envelope.
(b) Find an expression for the probability of bit error as a function of the average received bit energy-to-noise ratio.
(c) Plot your results in part (b) for different values of σ_Ω.

5.7 (Computer Exercise). This problem requires that you first complete the computer exercise in Problem 2.46, wherein you will construct a Ricean fading simulator. The objective of this question is to evaluate the performance of BPSK signaling on a Ricean fading channel through computer simulation.

Suppose that one of the two possible signal vectors $\tilde{s}_0 = -\tilde{s}_1 = \sqrt{2E_h}$ are sent where $E_h = E_b$ is the transmitted bit energy. Assuming ideal coherent detection, the received signal vector is

$$\tilde{r} = \alpha\tilde{s}_i + \tilde{n},$$

where α is a Ricean distributed random variable and $\tilde{n}$ is a zero-mean complex Gaussian random variable with variance N_o. For a given α, the probability of bit error is

$$P_b(\gamma_b) = Q\left(\sqrt{2\gamma_b}\right),$$

where $\gamma_b = \alpha^2 E_b/N_o$. The probability of bit error with Ricean fading is

$$P_b = \int_0^\infty Q\left(\sqrt{2\gamma_b}\right) p(\gamma_b)\mathrm{d}\gamma_b.$$

(a) Evaluate the bit error probability by using computer simulation, where α is generated by the Ricean fading simulator that you developed in Problem 2.46. Assume that the value of α stays constant for a bit duration, i.e., update your fading simulator every T seconds, where T is the bit duration. Assume $f_m T = 0.1$.

(b) Plot the simulated bit error probability, P_b, against the average received bit energy-to-noise ratio $\bar{\gamma}_b = \mathrm{E}[\alpha^2]E_b/N_o$. Show your results for $0.5 < P_b < 10^{-3}$ and for Rice factors $K = 0, 4, 7$, and 16. *Note: To adjust $\bar{\gamma}_b$ you will need to adjust the value of Ω_p in your fading envelope generator.*

5.8. Consider a non-orthogonal coherent binary FSK system with the bandpass waveforms

$$s_1(t) = A\cos(2\pi f_c t)\ ,\ \ 0 \le t \le T$$
$$s_2(t) = A\cos(2\pi(f_c + \Delta_f)t)\ ,\ \ 0 \le t \le T$$

and assume that $f_c T \gg 1$.

(a) Show that the correlation between the bandpass waveforms is given by

$$\rho = \frac{1}{E}\int_0^T s_1(t)s_2(t)dt = \mathrm{sinc}(2\Delta_f T)$$

where E is the energy in the waveforms.

(b) What is the value of Δ_f that minimizes the probability of symbol error?

(c) For the value of Δ_f obtained in part (b), determine the increase in the received bit energy-to-noise ratio, γ_b, required so that this coherent FSK system has the same bit error probability as a coherent binary PSK system.

5.9. OFDM systems are known to be resilient to timing errors. Consider the following OFDM waveform with a cyclic prefix

$$\tilde{s}_g(t) = A\sum_n b(t - nT_g, \mathbf{x}_n),$$

where

$$b(t, \mathbf{x}_n) = u_{\alpha_g T}(t + \alpha_g T)\sum_{k=0}^{N-1} x_{n,k} e^{j\frac{2\pi k(t+T)}{NT_s}} + u_T(t)\sum_{k=0}^{N-1} x_{n,k} e^{j\frac{2\pi kt}{NT_s}},$$

and $T = NT_s$ and $T_g = (1 + \alpha_g)T$. Suppose the waveform $\tilde{s}_g(t)$ is sampled every T_s seconds. For the nth OFDM symbol, this yields the sample sequence $\{X_{n,m}\}_{m=0}^{N-1}$, where

$$X_{n,m} = \tilde{s}(-\alpha_g T + nT_g + mT_s + \Delta_t),$$

and Δ_t is a timing offset. For the nth OFDM symbol an FFT is taken on the sample sequence $\{X_{n,m}\}_{m=0}^{N-1}$.

(a) Suppose that the timing offset Δ_t lies in the interval $(0, \alpha_g T)$ such that the samples $\{X_{n,m}\}_{m=0}^{N-1}$ all belong to the nth OFDM symbol. Determine the FFT coefficients.

(b) Now suppose that the timing offset Δ_t lies outside the interval $(0, \alpha_g T)$, such that the samples $\{X_{n,m}\}_{m=0}^{N-1}$ do not all belong to the nth OFDM symbol. Determine the FFT coefficients.

5.10. Consider the following OFDM waveform with a cyclic suffix and a carrier frequency offset Δ_f:

$$\tilde{s}_g(t) = A\sum_n b(t - nT_g, \mathbf{x}_n),$$

where

$$b(t, \mathbf{x}_n) = u_T(t)\sum_{k=0}^{N-1} x_{n,k}\exp\left\{j2\pi\left(\frac{k}{NT_s} + \Delta_f\right)t\right\}$$
$$+u_{\alpha_g T}(t - T)\sum_{k=0}^{N-1} x_{n,k}\exp\left\{j2\pi\left(\frac{k}{NT_s} + \Delta_f\right)t\right\},$$

$T = NT_s$ and $T_g = (1 + \alpha_g)T$. The waveform $\tilde{s}_g(t)$ is sampled every T_s seconds. For the nth OFDM symbol, this yields the sample sequence $\{X_{n,m}\}_{m=0}^{N-1}$, where

$$X_{n,m} = \tilde{s}(nT_g + mT_s).$$

An FFT is taken on the sample sequence $\{X_{n,m}\}_{m=0}^{N-1}$.

Show that the FFT coefficients (in absence of noise) can be written as

$$Z_{n,i} = \text{FFT}\{X_{n,m}\} = \eta x_{n,i} + c_i,$$

where

$$\eta = A \left\{ \frac{\sin\left(\pi N \Delta_f T_s\right)}{N \sin\left(\pi \Delta_f T_s\right)} \right\} e^{j\pi(N-1)\Delta_f T_s}$$

and

$$c_i = A \sum_{\substack{m=0 \\ m \neq i}}^{N-1} x_{n,m} H(m,i)$$

is the random ICI term, where

$$H(m,i) = \left\{ \frac{\sin\left(\pi\left(m - i + N\Delta_f T_s\right)\right)}{N \sin\left(\pi\left(m - i + N\Delta_f T_s\right)/N\right)} \right\} e^{j\pi\left(\frac{N-1}{N}\right)\left(m - i + N\Delta_f T_s\right)}.$$

5.11. Suppose that the average bit energy-to-noise ratio, $\bar{\gamma}_b$, in a cell is uniformly distributed between 12 and 16 dB. Calculate the average probability of bit error in the cell assuming that there is also Rayleigh fading, and binary DPSK signaling is used.

5.12. Consider the differentially coherent receiver shown in Fig. 5.18. Show that the pdf of U_n is given by (5.155).

5.13. Consider a system that uses M-ary orthogonal modulation with non-coherent detection. The error probability on an AWGN channel is known to be

$$P_b = \frac{M}{2(M-1)} \sum_{k=1}^{M-1} \frac{(-1)^{k+1}\binom{M-1}{k}}{k+1} \exp\left\{-\frac{k\gamma_s}{(k+1)}\right\},$$

where $\gamma_s = \alpha^2 E_s/N_o$ is the received *symbol*-energy-to-noise ratio.

(a) Derive the corresponding expression for the probability of bit error on a slow flat Rayleigh fading channel. Express your result in terms of the average received *bit*-energy-to-noise ratio, $\bar{\gamma}_b$, and simplify to closed form.
(b) Repeat part (a) for a slow flat Ricean fading channel. Simplify as much as possible.

5.14. Consider binary CPFSK modulation with modulation index $h \leq 0.5$. Compute the minimum squared Euclidean distance between any pair of bandpass waveforms as given by

$$D^2_{\text{min}} = \lim_{n\to\infty} \min_{i,j} \int_0^{nT} \left(s(t;\mathbf{x}^{(i)}) - s(t;\mathbf{x}^{(j)})\right)^2 \mathrm{d}t,$$

where $s(t;\mathbf{x}^{(i)})$ and $s(t;\mathbf{x}^{(j)})$ are the two bandpass signals whose phase trajectories diverge at time $t = 0$ and merge sometime later. What is the pairwise error probability between two such signals?

5.15. The squared Euclidean distance between a pair of CPM bandpass waveforms, $s(t;\mathbf{x}^{(i)})$ and $s(t;\mathbf{x}^{(j)})$, is

$$D^2 = \int_0^{\infty} \left(s(t;\mathbf{x}^{(i)}) - s(t;\mathbf{x}^{(j)})\right)^2 \mathrm{d}t.$$

Show that

$$D^2 = 2(\log_2 M)E_b \frac{1}{T}\int_0^{\infty} \left(1 - \cos \Delta_\phi(t)\right) \mathrm{d}t,$$

where M is the symbol alphabet size, E_b is the energy per bit, and $\Delta_\phi(t)$ is the phase difference between the two signals.

5.16. Construct a differential detector for MSK signaling. Obtain an expression for the probability of bit error for differentially detected MSK on an AWGN channel.

5.17. Suppose that GMSK signaling is used. Unfortunately, the GMSK pulse is non-causal and, therefore, a truncated version of the pulse is employed, i.e., the time domain pulse is

$$h_f(t) = \frac{1}{2T}\left(Q\left(\frac{t/T - 1/2}{\sigma}\right) - Q\left(\frac{t/T + 1/2}{\sigma}\right)\right) \mathrm{rect}\left(\frac{t - L_T T}{2L_T T}\right),$$

where

$$Q(\alpha) = \int_{\alpha}^{\infty} \frac{1}{\sqrt{2\pi}} \mathrm{e}^{-x^2} \mathrm{d}x \tag{5.204}$$

$$\sigma^2 = \frac{\ln 2}{4\pi^2 (BT)^2}. \tag{5.205}$$

Compute the maximum value of the ISI term in (4.149) as a function of the normalized filter bandwidth BT when $L_T = 3$.